

Impact of conjugated polymer addition on the properties of paraffin–asphaltene blends for heat storage applications: Insight from computer modeling and experiment

Cite as: J. Chem. Phys. **157**, 194702 (2022); <https://doi.org/10.1063/5.0122116>

Submitted: 22 August 2022 • Accepted: 25 October 2022 • Accepted Manuscript Online: 26 October 2022 • Published Online: 15 November 2022

 S. V. Larin,  V. V. Makarova,  S. N. Gorbacheva, et al.



View Online



Export Citation



CrossMark

ARTICLES YOU MAY BE INTERESTED IN

[Trajectory surface-hopping study of 1-pyrazoline photodissociation dynamics](#)

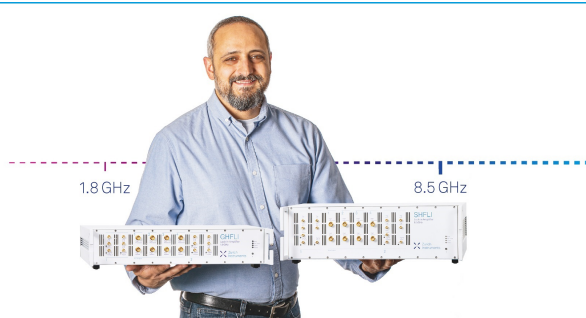
The Journal of Chemical Physics **157**, 194302 (2022); <https://doi.org/10.1063/5.0114698>


[Gas permeation rates of ultrathin graphite sealed SiO₂ cavities](#)

The Journal of Chemical Physics **157**, 191101 (2022); <https://doi.org/10.1063/5.0122356>


[Relativistic effects on electronic pair densities: A perspective from the radial intracule and extracule probability densities](#)

The Journal of Chemical Physics **157**, 194301 (2022); <https://doi.org/10.1063/5.0127190>



Trailblazers. 

Meet the Lock-in Amplifiers that measure microwaves.

 Zurich Instruments [Find out more](#)

Impact of conjugated polymer addition on the properties of paraffin–asphaltene blends for heat storage applications: Insight from computer modeling and experiment

Cite as: J. Chem. Phys. 157, 194702 (2022); doi: 10.1063/5.0122116

Submitted: 22 August 2022 • Accepted: 25 October 2022 •

Published Online: 15 November 2022



S. V. Larin,^{1,a)} V. V. Makarova,^{1,2} S. N. Gorbacheva,^{1,2} M. R. Yakubov,³ S. V. Antonov,^{1,2} N. I. Borzdun,¹ A. D. Glova,¹ V. M. Nazarychev,¹ A. A. Gurtovenko,¹ and S. V. Lyulin¹

AFFILIATIONS

¹ Institute of Macromolecular Compounds, Russian Academy of Sciences, Bolshoi Prospekt V.O. 31, St. Petersburg 199004, Russia

² A.V. Topchiev Institute of Petrochemical Synthesis, Russian Academy of Sciences, Leninsky pr. 29, Moscow 119991, Russian Federation

³ Federal Research Center Kazan Scientific Center, Russian Academy of Sciences, Lobachevskogo str. 2/31, Kazan 420111, Russian Federation

^{a)} Author to whom correspondence should be addressed: selarin@macro.ru

ABSTRACT

Adding carbon nanoparticles into organic phase change materials (PCMs) such as paraffin is a common way to enhance their thermal conductivity and to improve the efficiency of heat storage devices. However, the sedimentation stability of such blends can be low due to aggregation of aromatic carbon nanoparticles in the aliphatic paraffin environment. In this paper, we explore whether this important issue can be resolved by the introduction of a polymer agent such as poly(3-hexylthiophene) (P3HT) into the paraffin–nanoparticle blends: P3HT could ensure the compatibility of aromatic carbon nanoparticles with aliphatic paraffin chains. We employed a combination of experimental and computational approaches to determine the impact of P3HT addition on the properties of organic PCMs composed of paraffin and carbon nanoparticles (asphaltenes). Our findings clearly show an increase in the sedimentation stability of paraffin–asphaltene blends, when P3HT is added, through a decrease in average size of asphaltene aggregates as well as in an increase of the blends' viscosity. We also witness the appearance of the yield strength and gel-like behavior of the mixtures. At the same time, the presence of P3HT in the blends has almost no effect on their thermophysical properties. This implies that all properties of the blends, which are critical for heat storage applications, are well preserved. Thus, we demonstrated that adding polyalkylthiophenes to paraffin–asphaltene mixtures led to significant improvement in the performance characteristics of these systems. Therefore, the polymer additives can serve as promising compatibilizers for organic PCMs composed of paraffins and asphaltenes and other types of carbon nanoparticles.

Published under an exclusive license by AIP Publishing. <https://doi.org/10.1063/5.0122116>

I. INTRODUCTION

Nowadays, one of the most important issues in the field of environmental protection is the economical use of energy resources, part of which is the reduction of heat losses in production and in residential premises. One of the strategic directions to save heat is the use of special devices—heat accumulators, allowing thermal energy storing and consuming as needed. One of the most promising types of heat accumulators are devices based on phase change materials

(PCMs), whose operation principle is based on the accumulation and release of heat in the process of phase transition such as melting and crystallization.^{1–3} Currently, the various classes of compounds characterized by sufficiently high heat transition, chemical stability and inertness, and relatively low cost can be used as phase change materials.⁴

Paraffins are considered as a promising basis for the production of organic phase change composite materials.^{1,5,6} Usually, paraffins represent a mixture of *n*-alkanes of various molecular weight. By

varying the molecular weight distribution of paraffins in a blend, it is possible to change the temperature interval of its phase change over a wide range, depending on the requirements of the application of PCM.^{5,7,8} Additionally, paraffins offer the advantages of high energy storage density, thermal and chemical resistance, non-toxicity, affordability and low cost,^{6,9} as well as a low tendency to supercooling during crystallization, which provides stability and reproducibility of the phase change temperature.^{10,11}

However, paraffins, like most organic phase change materials, have a significant drawback that complicates their use in thermal accumulators: their low thermal conductivity.^{1–3,7} This leads to a decrease in the efficiency of thermal accumulators based on paraffins, as it slows down the processes of accumulation and release of thermal energy. In this regard, one of the main problems, the solution of which is necessary for the practical use of paraffins in thermal accumulators, is to increase their thermal conductivity.

In order to increase the thermal conductivity of paraffin-based PCMs, nanoparticles with high thermal conductivity, such as metallic or carbon nanoparticles, are most commonly added.^{2,3} The advantages of using carbon nanoparticles compared to metallic ones are their lower density and better dispersibility and stability in the PCM volume.² In particular, the thermal conductivity of paraffin-based PCMs has been shown to increase when carbon nanotubes,^{12–14} nanofibers,¹² graphene,^{15–17} graphite particles,^{18–21} and asphaltene molecules are introduced into them.^{22,23} It was shown that graphene-like nanoparticles (e.g., nanographite) have a greater influence on the thermal conductivity of PCM compared to nanofibers and nanotubes because of their low surface resistance and greater aspect ratio.^{2,12,17,18} So, in the work of Goli *et al.*,¹⁷ by introducing 20 wt. % graphene into paraffin it was possible to achieve an extreme increase in the thermal conductivity of paraffin up to 45 W/(m K), which was 180 times higher than the thermal conductivity of unfilled paraffin 0.25 W/(m K). Zhao *et al.*²¹ reported increase in PCM thermal conductivity up to 1695% compared with the paraffin using expanded graphite as a filler. However, in most cases, the addition of carbon nanoparticles leads to a significantly lower increase in the thermal conductivity of PCMs. The addition of only 0.3 wt. % graphene in beeswax resulted in an increase in the thermal conductivity of the mixture up to 2.89 W/(m K).¹⁵ In the study of Li,¹⁸ the thermal conductivity of paraffin was increased to 0.94 W/(m K) by the addition of nanographene particles. Moreover, in a number of works, the addition of carbon nanoparticles into paraffins led to insignificant changes in the thermal conductivity of materials. For example, in the work of Liu and Rao¹⁶ for paraffin mixtures containing 2 wt. % of graphene or exfoliated graphite, the thermal conductivity was 0.46 and 0.41 W/(m K), respectively, and in the study of Karaipekli,¹³ the addition of 1 wt. % of carbon nanotubes increased the thermal conductivity of paraffin only to 0.28 W/(m K).

The most significant problem when using carbon nanoparticles to increase the thermal conductivity of PCM is their tendency to aggregate, caused by strong π - π interactions between the macrocyclic fragments of their molecules.^{2,22} Aggregation of filler particles and subsequent phase separation in PCM leads to a decrease in their thermal conductivity and, consequently, a decrease in efficiency. At the same time, nanoparticle aggregation and nanoparticle percolation cluster formation are the key factors affecting the thermal conductivity of the material, since they form the phonon transfer

pathways necessary to increased thermal conductivity in the blends. Thus, the use of nanoparticles, including asphaltenes, to increase the efficiency of paraffin-based PCM requires solving two opposing problems: (1) increasing the sedimentation stability of nanoparticle dispersions and aggregation stability of nanoparticles in the mixture volume, including by increasing their compatibility with paraffins, and (2) providing heat transfer pathways between nanoparticles to increase the thermal conductivity of the mixture by forming a percolation cluster between them.

To solve such problems, the addition of polymers with both aromatic and aliphatic fragments in their structure to paraffin-based PCM containing carbon nanoparticles can be performed. Aromatic nanoparticles can form agglomerates with such polymers due to π - π interactions, and the polymer aliphatic groups will contribute to the compatibility of the aggregates with the paraffin. In the case of polymers having conjugated main chain, such additives will contribute to the formation of heat transfer pathways in the mixture, since polymers with a high degree of conjugation in the main chain have rather high values of thermal conductivity up to 0.37 W/(m K).^{24,25} One of the possible classes of polymers possessing a conjugated main chain with grafted aliphatic side chains are polyalkylthiophenes, among which poly(3-hexylthiophene) (P3HT) is the best known and widely used in organic electronics^{26,27} as the mixtures with various carbon nanoparticles,^{28–30} including asphaltenes.^{31,32}

At present, polymers are mainly used for PCM production as a carrier for the form-stable PCMs.^{7,24,33} Less frequently, polymers, such as polyethylene glycol or polyurethanes, act as phase change materials themselves.^{7,24} However, there are currently no studies that investigate the addition of small amounts of polymers to paraffin-based PCM to improve the phase change material properties. This is the aim of the presented study, in which we have analyzed, using both experimental and theoretical methods, the effect of P3HT introduction on the critical properties of paraffin-based PCM, viz., phase transition temperature and heat and the distribution and aggregation stability of filler particles in the blends.

As a continuation of our previous studies, we consider paraffin-based PCM filled with asphaltenes, relatively cheap by-products of deep oil refining.^{34,35} The chemical structure of their molecules can vary widely, but their common feature is the presence of one or more linked fragments containing a sufficiently large polycyclic aromatic core with short peripheral aliphatic groups.³⁴

Because of this feature of the chemical structure, asphaltene molecules can be considered as small fragments of graphene and used, like other carbon nanoparticles, to produce composite materials with improved mechanical and thermal properties,³⁵ for surface modification of carbon materials,³⁵ as promising acceptor materials in organic electronics.^{31,36,37} In addition, our previous studies have shown the possibility of using asphaltenes to improve the thermal conductivity of paraffin-based PCM, both by means of computer simulations,²³ and by experimental studies.²²

In our previous study, we performed computer simulations of the blends of *n*-eicosane with asphaltenes of two types: asphaltenes containing short aliphatic side chains attached to a polycyclic aromatic core and modified asphaltenes with the aliphatic groups removed.²³ The simulation results showed that the addition of asphaltenes with aliphatic side groups into paraffin leads to the creation of blends with a uniform distribution of small asphaltene

aggregates in the volume of the system. At the same time, the addition of such asphaltenes does not increase the thermal conductivity of the blend as compared to unfilled paraffin. Meanwhile, modified asphaltenes with removed aliphatic groups form extended columnar structures in the blends with paraffins, which can act as heat transfer pathways in the blends. Indeed, simulations have shown at least a twofold increase in the thermal conductivity coefficient of liquid paraffin at the maximum considered concentration of asphaltenes in the blend.

Experimental investigation of paraffin–asphaltene blends with different content of aliphatic and aromatic groups²² confirmed that an increase in the aromaticity degree of asphaltene molecules leads to an increased degree of aggregation and heterogeneous distribution of asphaltenes in the blend. This, in turn, led to a slight increase in the thermal conductivity of the blends compared to the unfilled paraffin. At the same time, for asphaltenes with a higher degree of aliphaticity, a lower propensity to form aggregates and a more uniform distribution of asphaltenes in the volume of the blend were found, which leads to a slight increase in the thermal conductivity of the material when adding 20 wt. % of asphaltenes to the paraffin. However, as the concentration of asphaltenes is further increased, the thermal conductivity of the materials decreases again due to the agglomeration of asphaltenes.

In this study, we will investigate the impact of P3HT introduction on the properties of paraffin-based PCM filled with asphaltenes in terms of the influence of additives on the PCM critical properties: (1) the temperature and heat of transition and (2) distribution and aggregation stability of filler particles in the volume of blends. The results of the studies will make it possible to determine how exactly the addition of polyconjugated polymers with aliphatic side groups affects the properties of paraffin-based PCM filled with carbon nanoparticles and show whether our proposed approach can be applied to improve the performance of such materials.

II. METHODS

A. Experimental materials and techniques

P-2 grade paraffin (Lukoil, Russia) with a melting point of 52–58 °C was used as a phase change material. P-2 grade paraffin is a solid petroleum paraffin of crystalline structure. It contains aliphatic hydrocarbons with a number of carbon atoms from 18 and above, mainly of normal structure. Paraffin of this grade is currently the purest and commercially available paraffin, which determines its choice as a model PCM.

Poly(3-hexylthiophene-2,5-diyl) (Ossila, UK) with a regioregularity of 94.2% and a molecular weight of $36 \cdot 10^3$ g/mol was used as a heat conducting polymer additive and compatibilizer for the paraffin-based blends (hereafter, P3HT).

The products of cracking (dealkylation) of native asphaltenes obtained from crude oil from the Ashalchinskoye field (Russia) were used as modifying additives for paraffin. To isolate native asphaltenes, 40 g of dehydrated crude oil was diluted with a 40-fold volume excess of *n*-hexane and thoroughly mixed. To ensure that the asphaltenes precipitate completely, the solution was stored in dark for 24 h. The asphaltene precipitate was then filtered, transferred to a filter paper cartridge, and placed in a Soxhlet apparatus

for washing asphaltenes to remove co-extracted maltenes. Then, the asphaltenes were washed with *n*-hexane until the solvent turned completely colorless.

Cracking of native asphaltenes was carried out with their solution (2 wt. %) in toluene. Cracking experiments were carried out in a 1-L high-pressure steel reactor (autoclave) of Parr Instrument Company. The pressure in the autoclave was maintained at 160 atm. The asphaltene solution was mixed for 20 min at 435 °C.

As a result of cracking, some of the asphaltenes precipitated as toluene-insoluble sediments on the bottom and walls of the autoclave. After washing with pure toluene and drying, this precipitate was referred to as CR-Coke. The other part of the cracked asphaltenes dissolved in toluene after removal of the solvent and drying was referred to as CR-A.

The structural features of the obtained products were evaluated by the following methods: Matrix Assisted Laser Desorption/Ionization (MALDI), electron paramagnetic resonance (EPR), x-ray photoelectron spectroscopy (XPS), and IR spectroscopy.

The molecular weight of the obtained asphaltenes and their molecular weight distribution were evaluated using the MALDI method. For this purpose, an UltraFlex III TOF/TOF mass spectrometer (Bruker Daltonik GmbH, Germany) was used. Measurements were performed in linear mode using a Nd:YAG laser with a wavelength of $\lambda = 355$ nm. The spectra were obtained with 30 ns acceleration delay and 25 kV accelerating voltage. The obtained data were processed using the FlexAnalysis 3.0 software (Bruker Daltonik GmbH, Germany).

According to MALDI data (Fig. S1 in the [supplementary material](#)), CR-A asphaltenes differ from native asphaltenes in having a lower molecular weight of about 700 g/mol, whereas native asphaltenes are mostly characterized by a molecular weight of about 1700 g/mol, and a narrower molecular weight distribution. As for the CR-Coke asphaltenes, they are characterized by a bimodal molecular weight distribution, and while the position of one peak corresponds approximately to the molecular weight of native asphaltenes, about 1700 g/mol, the second peak corresponds to very low molecular weight values, about 200 g/mol.

EPR spectra were recorded on the Elexsys E 500 spectrometer (Bruker, Germany). For the analysis, quartz glass ampoules with an inner diameter of 3 mm were fixed in the center of the EPR spectrometer's resonator. The ampoules were densely filled with the sample to a height of 13–14 mm, corresponding to the resonator's maximum sensitivity range. The number of free stable radicals (FSRs) was estimated by the intensity of a single line in the center of the spectrum ($g = 2.003$). The number of vanadyl complexes (VCs) was estimated by the intensity of the $+1/2$ line adjacent to the FSR line in the range of a weaker magnetic field. The FSR and VC contents (in relative spin/g) were determined as the line intensities of the studied sample were compared with the reference signal intensity.

Two types of intense paramagnetic particle signals are revealed when examining the structure of asphaltenes by EPR: free stable radicals (FSRs) and vanadyl complexes (VCs), Fig. S2 in the [supplementary material](#). The FSR signal arises due to the delocalization of unpaired electrons on carbon π -systems and, thus, their content reflects the degree of condensation of polyaromatic structures of asphaltenes. The FSR concentration is significantly higher for the CR-Coke sample.

The XPS studies were performed on PHI 5000 Versa Probe II spectrometer (ULVAC-PHI, Inc., USA). Monochromatic Al K α radiation ($h\nu = 1486.6$ eV), with power of 50 W and diameter of 200 μm , was used as the excitation source. The analyzer's transmittance energy was 23.5 eV and its collection density was 0.2 eV/step.

A high content of functional groups containing heteroatoms according to XPS data is observed in the CR-A sample (Table I). These are mainly C–OH/C–O–C and C=O groups, as well as $-\text{SO}_3\text{H}$ groups (which include 5 wt. % of all sulfur) and $-\text{S–O/H}$ (20 wt. % of all sulfur). Most of the sulfur for the CR-A sample is in the form of R–S groups in the thiophene form, and nitrogen is represented in this case as a part of vanadyl porphyrins.

CR-Coke asphaltenes contain 82 wt. % carbon in the graphite-like sp^2 -form, and sulfur atoms are mainly located in the center of the graphite lattice with substitution of carbon atoms in the cycles and partially in the R– SO_3H group. Nitrogen atoms are present in pyrrole cycles, in vanadylporphyrin complexes, and in pyridine cycles incorporated into the graphite lattice.

To identify the functional groups of the obtained asphaltenes, the infrared spectroscopy method was used. For this purpose, a Vector-22 IR-Fourier spectrometer (Bruker, Germany) with the optical resolution of 4 cm^{-1} was used. The spectra of the compounds were recorded in the range of 4000–400 cm^{-1} . Samples were prepared in tablets with KBr (Acros Organics, 206391000). To study the structural and group composition of samples, the following spectral coefficients were calculated: $\text{Al}^\circ = (D_{720} + D_{1375})/D_{1600}$ (aliphaticity), $\text{Ar}^\circ = D_{1600}/D_{720+1380}$ (aromaticity), $\text{Br}^\circ = D_{1380}/D_{720}$ (branching), $\text{C}_n = D_{1600}/D_{740+860}$ (degree of condensation), $\text{Ox} = D_{1700}/D_{1600}$ (degree of oxidation), and $\text{Sl}^\circ = D_{1030}/D_{1600}$ (degree of sulfonation) the same way as it was done in the previous study.²² The data obtained are shown in Table II, from which it can be seen that, in contrast to native asphaltenes, the CR-A and CR-Coke products are characterized by increased condensation and aromaticity and contain fewer aliphatic substituents. These results are consistent with those obtained by other methods.

The blends based on paraffin and poly(3-hexylthiophene) were prepared by introducing P3HT in amounts of 1, 5, 10, and 15 wt. % into the molten paraffin at 180 °C and constant stirring on a magnetic stirrer. Compositions containing additional asphaltenes were prepared by injecting 5 wt. % of CR-A and CR-Coke samples at 120 °C with stirring on a magnetic stirrer for 30 min.

The thermophysical properties of the blends were studied by modulated differential scanning calorimetry (MDSC) on an MDSC 2920 calorimeter (TA Instruments, USA). DSC thermograms were

TABLE II. Spectral coefficients derived from IR spectroscopy data for native asphaltenes, CR-A samples, and CR-Coke samples.

Samples	Al	Ar	Br	Cn	Ox	Sl
Native	2.22	0.44	2.0	0.37	0.30	0.48
CR-A	2.19	0.75	0.94	0.53	0.38	0.56
CR-Coke	1.37	0.77	1.07	0.96	0.31	1.17

obtained in the temperature range from 0 to 100 °C at a heating/cooling rate of 5 °C/min. The degree of crystallinity of the samples was estimated from the ratio of the experimentally determined melting heat of the material to the melting heat of eicosane (284.2 J/g)³⁸ corrected for the mass fraction of paraffin in a particular system.

The influence of fillers on the structural properties of paraffin was studied by x-ray diffraction analysis on a Rotaflex D/max-RC x-ray diffractometer (Rigaku, Japan) at a wavelength of 0.154 nm. Diffractograms were recorded in a range of 2 θ angles of 3–70° with a step of 0.04° and a recording rate of 4°/min.

The compatibility of paraffin with P3HT was investigated by the method of laser microinterferometry.^{39,40} A 70 μm -thick polymer film was preformed by pressing at 200 °C. The film sample was placed between glasses, a diffusion cell was assembled, heated to 60 °C, and molten paraffin was added dropwise so that it was brought into contact with the P3HT film. The measurements were performed in a mode where the temperature was increased and decreased stepwise from 20 to 220 °C. The moment of contact of the components was considered the beginning of the diffusion process. A modular KLM-A532-15-5 laser with a wavelength of 532 nm was used as a light source.

Optical micrographs of the samples were obtained at room temperature using a microscope equipped with a Levenhuk digital video camera.

The rheological measurements of the blends of paraffin with P3HT and asphaltenes were performed on a rotational rheometer DHR-2 (TA Instruments, USA) at 80 °C using a cone-plane measuring unit (cone diameter was 25 mm, the angle between the cone surface and the plane was 2°). The measurements were carried out in two modes: 1) studying the steady-state flow with stepwise increase of the shear rate from 10^{−3} to 1000 s^{−1} and 2) obtaining the frequency dependence of the linear elasticity moduli and losses at a deformation amplitude of 0.1%–10% and variation of angular frequency from 0.0628 to 628 rad/s.

The measurements of thermal conductivity of paraffin, P3HT, asphaltenes, and their blends were carried out at 20 °C using a KITT-Nanocomposite equipment (KB “Teplofon”, Russia).⁴¹ Samples were preliminarily prepared in the form of tablets with a diameter of 10 mm and a thickness of 5 mm. Asphaltene tablet samples were prepared by compacting asphaltene powders in a mold at room temperature under light pressure. Then, the samples were placed into a measuring cell made of neutral material. The method of measurement consisted of uniform preheating of the sample and then its monotonous cooling from one side using a Peltier element with calculation of the value of thermal conductivity using the temperature difference at the edges of the sample and the value of heat flow.

TABLE I. Weight percentages of elements at the surface of asphaltenes according to XPS.

Samples	Content, wt. % (surface)			
	C	N	O	S
Native	93.0	1.0	2.1	3.6
CR-A	91.8	2.0	3.2	2.9
CR-coke	90.2	2.1	4.9	2.9

B. Simulation models and methods

Atomistic simulations of ternary paraffin/asphaltene/P3HT blends were performed to study the molecular mechanisms determining the effect of P3HT addition on the properties of paraffin-based phase change materials filled with asphaltenes. Paraffin *n*-eicosane ($C_{20}H_{42}$), Fig. 1(a), was used as a main component of the blends studied. *n*-eicosane is one of the most promising materials for domestic use in thermal storage devices due to the fact that its melting point (37°C)^{8,42} is close to the physiological one. As the paraffin used in the experimental part of the study is a blend of hydrocarbons of variable composition, its exact reproduction in the simulation is difficult to achieve in practice. Meanwhile, *n*-eicosane is close to the lower molecular weight limit of hydrocarbons included in the P-2 grade paraffin composition, which makes *n*-eicosane a good model molecule for such paraffins. In addition, the structural and thermal properties of *n*-eicosane^{43–45} and its mixtures with asphaltenes have been previously studied.²³

Regioregular poly(3-hexylthiophene), Fig. 1(b), having a conjugated main chain with the grafted aliphatic groups, was considered as a polymer additive to the mixtures of paraffin with asphaltenes. The degree of polymerization of P3HT used in the simulation was $N_p = 40$, which corresponds to the polymer regime and is commonly used in simulation of this polymer,^{46–49} including its blends with asphaltenes.³²

In this work, as well as in an earlier study of the blends of paraffin with asphaltenes,²³ the blends containing two types of asphaltene molecules were investigated, Figs. 1(c) and 1(d). Although the complex chemical composition of asphaltenes⁵⁰ makes it very difficult to build a model of asphaltenes in computer simulations,^{51,52} we were guided by two key factors in choosing the specific chemical structures: the relative simplicity of the model and its approbation in other studies.

There are many different asphaltene structures that meet these criteria and can therefore be used in simulations. As typical representatives, one can mention the structure proposed by Mullins³⁴ and further developed by Li and Greenfield⁵³ as well as the model of an “island” asphaltene molecule proposed by Headen.^{54,55} Mullins’s model asphaltene contains sulfur as a heteroatom in the fused core, whereas heteroatoms in Headen’s model are located in the side chains only. At the same time, elemental analysis of experimental asphaltene samples presented above shows that the asphaltenes should contain heteroatoms in their aromatic core.

Thus, the structure proposed by Mullins³⁴ was chosen as the basic model of asphaltenes in our research. It represents a small aromatic nucleus with one heteroatom of sulfur, to which the aliphatic groups are grafted, Fig. 1(c). Hereafter, this type of molecule will be referred to as Asp. Calculation of the solubility of Asp in organic solvents confirmed that this model corresponds to the definition of asphaltenes, i.e., the molecules are soluble in toluene and insoluble in heptane.⁵⁶ In recent years, it has been successfully used to study the oil–water interface⁵⁷ and asphalt.^{53,58,59} Importantly, this model was also used in our recent study of paraffin–asphaltene blends.²³ Moreover, since the main goal of the present paper is to study the impact of polymer addition on the properties of paraffin–asphaltene systems, the choice of our asphaltene molecule is well justified as it allows us to link our findings directly with earlier computational results.

The choice of the second model asphaltene molecule representing Asp with the removed aliphatic groups [hereafter referred to as Asp-Core, Fig. 1(d)] is based on the following factors. It is known that the formation of “stacked” structures of aromatic molecules caused by π – π interactions between them leads to an increase in the thermal conductivity of materials.^{60,61} Thus, to increase the thermal conductivity of PCM when asphaltenes are added to them, the

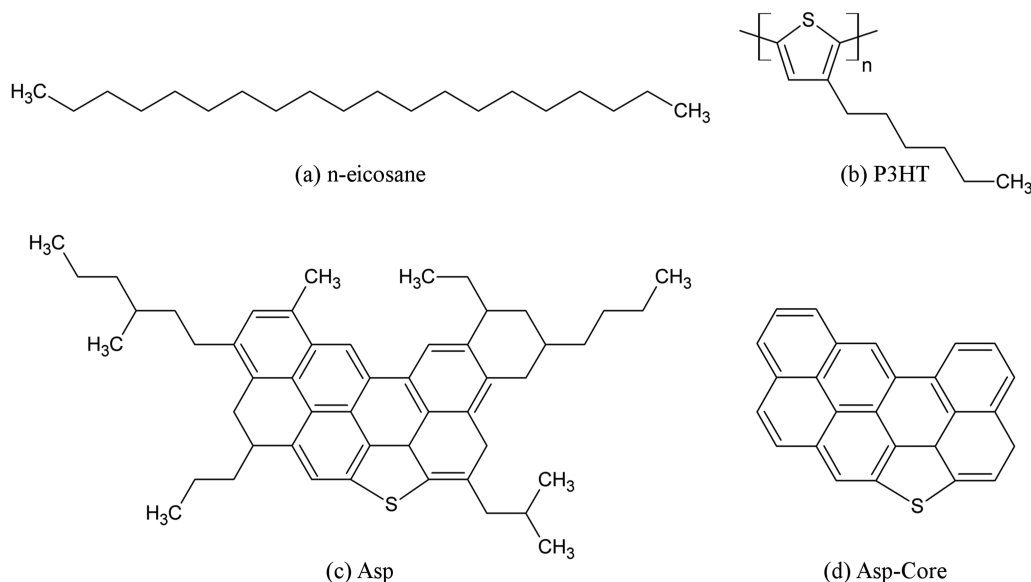


FIG. 1. Chemical formulas of components of blends studied using computer simulations: (a) *n*-eicosane; (b) poly-(3-hexylthiophene), P3HT; (c) model asphaltene with aliphatic side groups (Asp); and (d) modified asphaltene with removed aliphatic groups (Asp-Core).

latter should form such structures stabilized by interactions between the aromatic nuclei of asphaltene molecules. However, it has been shown that asphaltene molecules containing aliphatic fragments form rather loose aggregates with a low degree of ordering.^{62–64} This is presumably due to the fact that aliphatic groups prevent the mutual orientation of aromatic nuclei and thus the formation of thermally conductive “stacked” aggregates.^{34,62} Indeed, in the study of Bian *et al.*, it was shown, based on experimental and theoretical studies, that alkylation of asphaltenes leads to a decrease in the aggregation of asphaltenes in solution.⁶⁵

Consequently, chemical modification of Asp by “removing” aliphatic fragments of asphaltene molecules, which can be realized using cracking,^{66,67} can lead to improved functional characteristics of PCM based on paraffin filled with asphaltenes as confirmed by the results of computer simulation performed using the Asp-Core model.²³ At the same time, experimental data show that increasing the degree of aromaticity of asphaltenes, although it increases their tendency to aggregate in paraffin, leads to a decrease in the homogeneity of their distribution in the mixture and, thus, does not cause a significant increase in the thermal conductivity of the material.²²

The molar mass of Asp and Asp-Core asphaltenes is 708 and 358 g/mol, respectively. The mass fraction of carbon atoms in the sp^2 -hybridization state is 41% for Asp and 87% for Asp-Core. The amount of heteroatoms (sulfur) in these two molecules differs by a factor of 2 and amounts to 4.5% in Asp and 9% in Asp-Core. It should be noted that, although the molecular weight of the model asphaltenes is smaller than that of the asphaltenes obtained in the experiment, the ratio between the molecular weight of Asp and Asp-Core is close to the difference between the most probable molecular weights of native asphaltenes and CR-A asphaltenes. At the same time, Asp molecules are close to native asphaltenes in terms of the ratio of different types of atoms, whereas Asp-Core is close to CR-A and CR-Coke.

Thus, the study of PCMs based on paraffin with two types of asphaltenes in the presence and absence of P3HT additive will allow us to determine the impact of the polymer with a conjugated main chain and grafted aliphatic groups and simultaneously asphaltene chemical structure on the phase change material properties, which is necessary to develop new types of PCMs and predict their properties.

All the investigated systems contained 500 *n*-eicosane molecules, as in the previous study investigating PCMs based on paraffin filled with asphaltenes,²³ and four P3HT chains with polymerization degree $N_p = 40$. In addition to paraffin and P3HT,

the ternary blends also included 99 molecules of one of the two types of asphaltene (Asp or Asp-Core).

The choice of the amount of P3HT chains introduced into the studied systems is related to the composition of the blends studied in the experiment. For a more correct comparison of the simulation results with the experimental data, the mass fraction of P3HT in the simulated systems (from 11 to 16 wt. %) was chosen to be close to the limiting mass fraction of the polymer in the blends studied in the experiment (15%).

The choice of the number of molecules in the considered systems was based on previously performed simulations of blends of paraffin with two types of asphaltenes, which showed that significant differences in the structure and properties of the blends, including thermal conductivity, are found when the blend contains 99 asphaltene molecules, which corresponded to 20% of the asphaltene mass fraction in the blend with paraffin.²³ For the blends considered in this study, the mass fraction of this number of asphaltene molecules is 29 wt. % (for Asp) or 17 wt. % (for Asp-Core). The considered asphaltene concentrations are higher than the concentrations used in the experiment. This is due to the fact that, the rather limited spatial and time scales are available for the investigation using all-atom molecular dynamics simulations. Increasing the concentration of nanoparticles in the considered systems makes it possible to accelerate their aggregation process and study the aggregation-related effects at the times available for simulation on the order of a few microseconds.

The list of systems, mass fraction of components, and number of atoms in each system are given in Table III. To determine the impact of P3HT on the properties of paraffin–asphaltene blends, results obtained for the systems containing P3HT were compared with data previously obtained from simulation of PCMs based on paraffin containing asphaltenes²³ as well as unfilled paraffin.⁴³

Computer simulations were performed using the molecular dynamics program implemented in the Gromacs software package.^{68–70} The GAFF force field⁷¹ was used to describe the investigated systems. This force field was successfully used previously to study the structure and properties of various systems containing paraffins,^{43–45} asphaltenes,^{56,65,72,73} and P3HT,^{74–78} including paraffin–asphaltene blends,²³ and P3HT with asphaltenes.³² Description of all molecules in the GAFF force field, including values of the atomic partial charges, was obtained using the ACPYPE program.^{79,80} Information on the partial charges and GAFF atom types of the P3HT is provided in the [supplementary material](#) (Fig. S3 and Table S1). The force field parameters of asphaltenes were published in our previous work.²³

TABLE III. Composition of the investigated systems and the mass fractions of their components.

Component	System composition (number of molecules/mass fraction, %)		
	Paraffin/P3HT	Paraffin/Asp/P3HT	Paraffin/Asp-core/P3HT
Paraffin (<i>n</i> -eicosane)	500/84	500/59	500/70
P3HT	4/16	4/11	4/13
Asp	...	99/29	...
Asp-core	99/17
Number of atoms in the system	35 008	46 294	38 869

To create the initial configurations of the investigated systems, P3HT, paraffin, and asphaltene molecules were randomly placed in a sufficiently large cubic cell, followed by a preliminary simulation that included compression of the system at $T = 177^\circ\text{C}$ (450 K) and pressure $P = 100$ bars for 5 ns and subsequent simulation at pressure $P = 1$ bar also for 5 ns. Preliminary simulations were performed using the Berendsen thermostat and barostat.⁸¹

The main simulation was performed for 3 μs at a temperature $T = 177^\circ\text{C}$ (450 K) and a pressure $P = 1$ bar. The temperature and pressure were kept constant using the Nose–Hoover thermostat^{82,83} and the Parrinello–Rahman barostat,⁸⁴ respectively. The P-LINCS method⁸⁵ was used to constrain bonds with hydrogen atoms. The PME method⁸⁶ was used to calculate the electrostatic interactions. The simulation was carried out with a time step of 2 fs using periodic boundary conditions.

For paraffin–asphaltene blends that do not contain P3HT, the simulation time for each of the investigated systems was 1 μs and the equilibration time was on the order of 100 ns.²³ The sizes of the polymer chains in the systems with P3HT significantly exceed the sizes of the individual asphaltene and *n*-eicosane molecules, so their equilibration time is significantly longer, on the order of 1.5 μs , which was determined by analyzing the time dependence of the P3HT chain sizes and their mean square displacement in the investigated systems (Fig. S4 in the [supplementary material](#)). In this regard, a significantly longer simulation time was necessary for the P3HT-containing systems as compared to the simulation time for the paraffin–asphaltene blends in order to obtain statistically reliable results. Thus, for each of the P3HT-containing blends, the simulation time was 3 μs .

To assess the thermophysical properties of the blends, viz., crystallization temperature and heat, as well as thermal conductivity in the crystalline state, simulations of cooling of the blends were performed from 177°C (450 K) to -23°C (250 K) with a cooling rate of 6×10^9 K/min, similar to the previous studies.²³ Cooling was performed stepwise with a temperature decrease by 10 K every 100 ns of the simulation. For each of the investigated systems, cooling was performed for three statistically independent configurations.

It has to be emphasized that the cooling rate can have a crucial influence on the crystallization and melting processes studied by molecular dynamics simulations. In our recent work,⁸⁷ we systematically explored this influence for the crystallization of *n*-eicosane (the same paraffin as in the present study). We showed

the existence of a certain threshold in the values of cooling rates (6×10^{11} K/min). At smaller rates, computer simulations are able to qualitatively reproduce the crystallization process in paraffins and the computational results are in line with experimental data. However, beyond this threshold, when cooling is too fast, a large part of the system is trapped in the supercooled liquid state. As a result, one has a systematic decrease in the fraction of crystalline domains in a paraffin sample with cooling rate, leading eventually to a complete lack of crystallization at low temperatures. The cooling rate used in the present study is much smaller than the above-mentioned threshold. Moreover, this cooling rate is very close to the state-of-the-art limit accessible through atomistic computer modeling.⁸⁸ Thus, we can conclude that the cooling rate chosen for our simulations allows us to obtain reliable data on phase transitions in the systems at hand.

The method based on equilibrium molecular dynamics (EMD)⁸⁹ has been used to calculate the thermal conductivity of the blends as in our previous studies.⁴⁴ In the EMD method, the thermal conductivity coefficient is determined by analyzing the autocorrelation function of heat flow (HFACF) using Green–Kubo equations.^{90,91} For this purpose, we simulated the paraffin/asphaltene/P3HT systems in the NVE ensemble for 1 ns, which allowed the heat flow in these systems to be calculated. The simulations were performed in the LAMMPS software package⁹² for which the studied systems were converted from the Gromacs representation to the LAMMPS format using the procedure developed by us. Next, the HFACF was calculated by averaging over each 10 ps time frame of the simulation⁹³ and the HFACF thus obtained, in turn, was used to calculate the thermal conductivity coefficient, which was averaged over the last 500 ps of the NVE ensemble simulation trajectory.⁴⁴

III. RESULTS

A. Thermophysical properties

Introduction of up to 5 wt. % P3HT into paraffin practically does not change its phase change temperature (Fig. 2), but it leads to a decrease in crystallinity by about 20% (Table IV). Repetition of the melting–crystallization cycles for the paraffin-based composition with 5 wt. % P3HT demonstrates the homogeneity of the system—the phase change temperatures and degree of crystallinity are maintained at the same values. Adding 5 wt. % P3HT into the

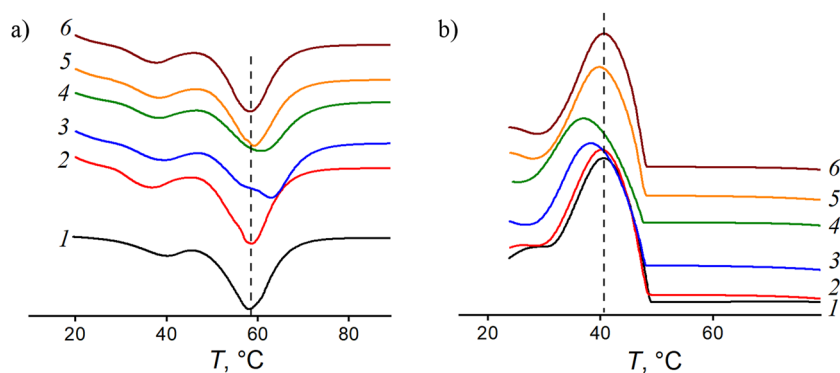


FIG. 2. DSC thermograms obtained by (a) heating and (b) cooling of pure paraffin (1) and blends containing 1 wt. % (2), 10 wt. % (3), and 15 wt. % (4) of P3HT; 5 wt. % of CR-A asphaltene and 5 wt. % of P3HT (5); and 5 wt. % of CR-Coke asphaltene and 5 wt. % of P3HT (6). Dashed lines correspond to the melting and crystallization temperatures of pure paraffin.

composition containing 5 wt. % CR-A or CR-Coke asphaltenes does not significantly change the behavior of the systems, contributing only to a slight increase in melting temperature by 1–2 °C [Fig. 2(a)]. At 10 and 15 wt. % P3HT content in paraffin, the melting point increases and the crystallization temperature decreases by 3–5 °C in comparison with that of pure paraffin, the shape of the peaks in the thermograms changes. These results indirectly indicate co-crystallization of the components.⁹⁴

In the computer simulation, the thermophysical characteristics of paraffin-based systems were determined based on the analysis of the temperature dependence of their density ρ and enthalpy H . The analysis for the dependence $\rho(T)$ (Fig. 3) allowed us to determine the crystallization temperature of the investigated systems (Table V) and assess the impact of P3HT introduction into blends.

The obtained data show that adding the modified Asp-Core asphaltenes to paraffin leads to an increase in the crystallization temperature of the blend by about 7 °C, which agrees well with the experimental data.²² However, the addition of P3HT to paraffin-based blends, as in the experiment, has little effect on the phase change temperature of the blends. Thus, for paraffin and its mixtures with Asp-Core asphaltenes, the crystallization temperature changed on adding P3HT by less than 0.5 °C, and for the blends with Asp-Core asphaltenes it decreased by 3.6 °C. The obtained differences in the crystallization temperatures of the blends correlate well with the experimental data.

It is worth noting that the paraffin crystallization temperature determined by computer simulations is higher than the experimentally determined crystallization temperature of *n*-eicosane, which is 37 °C.⁸ This is generally a characteristic of paraffin modeling using full-atomic models, which leads to an overestimation of the paraffin crystallization temperature.⁴³

The density of P3HT-containing systems in the melt is higher than that of mixtures containing no polymer additive, which is due to the higher density of pure P3HT compared to that of paraffin. However, at temperatures below the crystallization temperature, the density of the systems containing P3HT and without it does not differ very significantly, and in the case of the blends containing

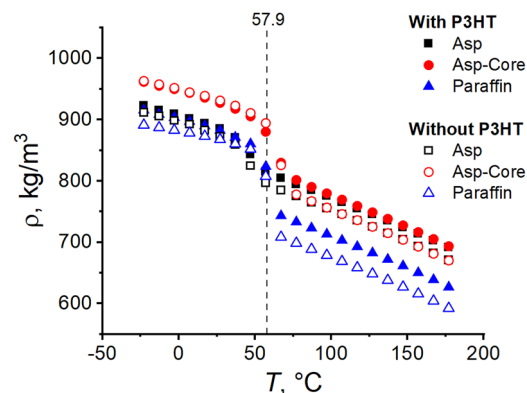


FIG. 3. Temperature dependence of the paraffin-based system density. The dashed line corresponds to the crystallization temperature of paraffin determined using simulation data.

Asp-Core asphaltenes, the introduction of P3HT does not lead to any change in the density of the blend in the crystallized state.

The maximum density of the blends containing Asp-Core asphaltenes is connected with a high degree of ordering of paraffin molecules in them. Indeed, as will be shown below, analysis of the paraffin structure in the studied systems at temperatures below the crystallization temperature indicates that the addition of P3HT leads to an increase in the degree of ordering of the paraffin molecules. However, for correct comparison of the results of computer simulation with experimental data, the degree of crystallinity should be determined using similar approaches. Since the degree of crystallinity in the experiment is estimated indirectly on the basis of data on the thermal impact of the phase change on the examined blends, it was decided to use a similar approach in the analysis of computer simulation data.

Thus, to estimate the thermal effect of crystallization and to directly compare the computer simulation data with the DSC results,

TABLE IV. Thermophysical properties of blends based on paraffin, P3HT, CR-A, CR-Coke.

Filler content (wt. %)C	Melting		Crystallization		Crystallization degree (%)
	T_m (°C)	ΔH_m (J/g)	T_{cr} (°C)	ΔH_{cr} (J/g)	
0 (pure paraffin)	58.2	198.5	40.7	210.0	69.8
1 (P3HT)	58.7	148.7	41.2	128.2	52.9
5 (P3HT)	57.6	141.6	41.1	136.9	52.4
Second heating-cooling cycle	56.8	141.5	41.2	136.9	52.4
Third heating-cooling cycle	56.6	139.2	41.0	137.1	51.6
Fourth heating-cooling cycle	56.7	140.3	41.1	137.2	52.0
Fifth heating-cooling cycle	56.7	140.6	41.2	137.5	52.1
Sixth heating-cooling cycle	56.6	139.9	41.3	136.9	51.8
10 (P3HT)	63.0	135.3	39.5	116.8	52.9
15 (P3HT)	61.1	121.6	38.4	98.2	50.3
5 (P3HT) + 5 (CR-A)	59.3	133.5	40.7	115.5	52.2
5 (P3HT) + 5 (CR-coke)	58.5	134.0	41.3	115.9	52.4

TABLE V. Temperature T_{cr} and enthalpy ΔH_{cr} of crystallization of paraffin-based systems determined by computer simulation and the degree of crystallinity of blends, K_{sim} .

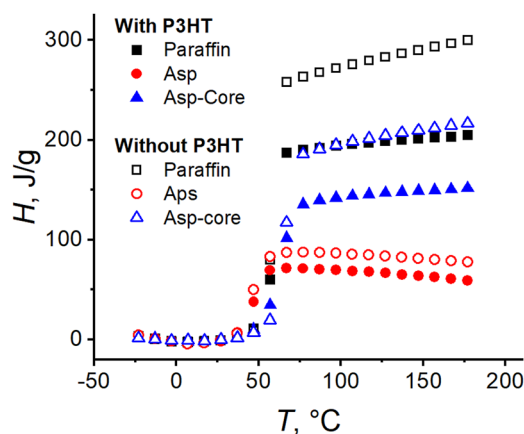
Type of asphaltene	T_{cr} (°C)		ΔH_{cr} (J/g)		K_{sim} (%)	
	With P3HT	Without P3HT	With P3HT	Without P3HT	With P3HT	Without P3HT
Without asphaltenes	57.6	57.9	187.0	258.1	66	91
Asp	45.0	44.9	69.4	83.1	24	29
Asp-core	61.0	64.6	135.4	185.8	48	65

the temperature dependence of the enthalpy of the investigated systems $H = E_{tot} + pV$ was determined, where E_{tot} is the total energy of the system, V is the modeling cell volume, and p is the pressure in the system. The obtained temperature dependence of the enthalpy of the studied systems (Fig. S5 in the [supplementary material](#)) were used to determine the heat of crystallization of the blends of paraffin with asphaltenes with and without the addition of P3HT.

To determine the heat of transition (crystallization or melting) for DSC, the temperature dependence of enthalpy is reduced to zero by subtracting the baseline from it.^{95,96} In our case, we also transformed the temperature dependence of enthalpy by subtracting the baseline corresponding to the linear approximation of the low-temperature region of dependence $H(T)$: from -23 to 37°C (Fig. 4). The crystallization heat ΔH_{cr} was then determined as the enthalpy value after an abrupt jump in the (reduced) $H(T)$ curves. The crystallization enthalpy values thus determined are shown in Table V.

The degree of crystallinity of the systems researched in the modeling K_{sim} was determined as the ratio of the enthalpy of crystallization of the system ΔH_{cr} to the enthalpy of crystallization of the ideal *n*-eicosane crystal $\Delta H_{paraf} = 284.2 \text{ J/g}$.³⁸

$$K_{sim} = \frac{\Delta H_{cr}}{\Delta H_{paraf}} \cdot 100\%.$$

**FIG. 4.** Temperature dependence of the enthalpy H after subtraction of the baseline corresponding to a linear approximation of the low-temperature region.

This definition allows us to compare the results of the computer simulation directly with the experimental data. The determined values of crystallinity degree, K_{sim} , are also given in Table V.

The results of computer simulation show good qualitative agreement with the experimental data both in their values of the enthalpy of crystallization of the blends and in the calculated degree of crystallization. Indeed, the introduction of P3HT both in unfilled paraffin and in the blends containing asphaltenes leads to a decrease in the degree of crystallinity of the material. Nevertheless, modeling shows that the decrease in crystallinity of the asphaltenes-containing blends is mainly due to the introduction of asphaltenes, while the addition of P3HT leads to a relatively small decrease in crystallinity compared to that of the polymer-free systems. At the same time, for a mixture of paraffin with P3HT, not containing asphaltenes, a considerable decrease in the degree of crystallinity in comparison with unfilled paraffin is observed. Such a change is connected with disturbance of the crystal structure of paraffin in the blend, which is expressed, as it will be shown below, in terms of increase in the quantity of crystal domains in the structure of paraffin when P3HT is added.

B. Structural properties

1. Crystallization of paraffin in blends when introducing P3HT

X-ray diffractograms of paraffin obtained at room temperature are typical for this material: In the range of angles from 3° to 15° , peaks characterizing the periodicity of the paraffin chains are observed, and in the range of 15° – 25° , peaks typical for the crystal lattice are observed (Fig. 5).⁴¹ X-ray diffractograms of P3HT indicate its crystallinity. The first peak in the diffractogram for P3HT at 5° corresponds to the plane (100), and its position is related to the lattice constant. The second peak localized in the 20° to 2θ region corresponds to the plane (010) and is related to the head-to-head packing of the P3HT chains.⁹⁷

The introduction of P3HT into the paraffin does not lead to significant changes in the structure of the paraffin [Fig. 5(a)]. The co-crystallization of components can be noted, as evidenced by disappearance of the paraffin reflex at 10° , accompanied by strengthening of the reflexes at angles 21.3° and 23.6° and preservation of all reflexes at angles above 30° .

The addition of 5 wt. % asphaltenes of different nature to paraffin/P3HT blends generally does not result in an apparent change in the reflex positions typical for the paraffin + 5 wt. % P3HT blend. However, it can be noted that the use of CR-Coke asphaltenes as

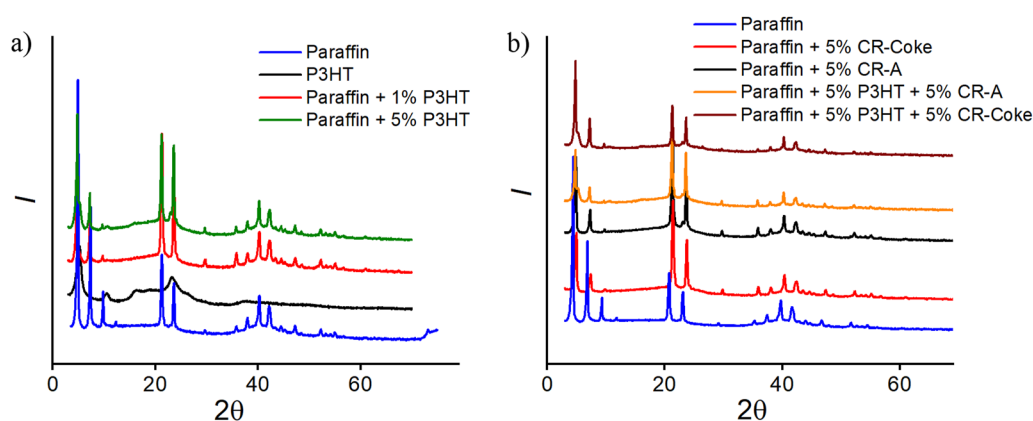


FIG. 5. X-ray diffractograms of blends based on paraffin filled with (a) poly(3-hexylthiophene) and (b) poly(3-hexylthiophene) and asphaltenes. The concentration of fillers is given in the legend inside the figures.

a filler leads to an increase in the intensity of the peak in the 5° region, characterizing the ordering of the chains, and a decrease in the intensity of the peak in the 20° region, responsible for the ordering of the crystal structure. However, the situation is reversed when CR-A asphaltenes are introduced into the system, which, in turn, contribute more to the ordering of the crystal lattice [Fig. 5(b)].

Thus, when using poly(3-hexylthiophene) as a filler for paraffin, co-crystallization of components is observed. At the same time, the introduction of asphaltenes into the obtained system has no significant effect on the crystallization of blends, which favorably affects their thermophysical properties.

2. P3HT compatibility with paraffin

Interferograms obtained by laser microinterferometry show no visible changes in the diffusion zone after contact of P3HT with paraffin at the melting temperature of paraffin; the area with P3HT looks dark and the interference bands on the paraffin side do not acquire a typical bend, indicating diffusion processes [Fig. 6(a)]. However, as the temperature approaches 180°C , dissolution of the polymer in the paraffin begins [Fig. 6(b)], the interference bands curve intensely, and the interfacial boundary disappears. According to the DSC data of P3HT (Fig. S6 in the [supplementary material](#)), this temperature interval precedes the beginning of the melting of the P3HT crystal phase. After cooling of the cell, crystals form not only on the paraffin side but also in the diffusion zone [Fig. 6(c)], indicating co-crystallization of the components as shown in the figure. Thus, the behavior of P3HT appears to be fully compatible with that of paraffin above 180°C .

Analysis of optical microphotographs of blends can also indirectly indicate co-crystallization of paraffin with P3HT. Figure 7 shows room temperature micrographs of blends containing 5% P3HT [Fig. 7(a)] with the addition of 5 wt.% CR-A [Fig. 7(b)] and CR-Coke [Fig. 7(c)]. The blend of paraffin with P3HT looks quite homogeneous—the dark (P3HT) and light (paraffin) areas are evenly distributed. Additional introduction of 5 wt.% asphaltenes does not violate the structure of the blends. The presence of

asphaltene agglomerates is observed of sizes up to $10\text{--}20\ \mu\text{m}$. At the same time, asphaltene agglomerates of noticeably larger sizes are observed in the absence of P3HT. Thus, the use of P3HT probably contributes to more homogeneous dispersion of asphaltenes in the paraffin matrix.

Computer simulations also confirm the co-crystallization of the polymer (primarily the aliphatic side chains) and paraffin in the P3HT–paraffin dual systems. Analysis of the instantaneous configuration of the investigated systems shows that the polymer chains are embedded in the domain structure of the paraffin crystal and, apparently, have an additional ordering effect on the paraffin. The representative snapshots are shown in Fig. 8.

Furthermore, comparison of snapshots for paraffin–asphaltene mixtures with and without P3HT shows different effects of P3HT addition on the distribution of Asp and Asp-Core molecules. In the case of Asp-containing mixtures, there are no sufficient changes visible in the distribution of asphaltene molecules upon addition of P3HT [Figs. 8(d) and 8(f)]; the Asp molecules are distributed almost uniformly over a simulation box. At the same time, addition of P3HT to the mixture of paraffin with Asp-Core results in sufficient condensation of asphaltenes on P3HT chains and also a certain decrease in the size of Asp-Core aggregates [Figs. 8(e) and 8(g)]. These observations are confirmed by the structural characteristics of asphaltene aggregates and pair distribution functions (see below).

To estimate the degree of ordering of the paraffin molecules in the studied blends, the number of ordered domains in the paraffin N_{domain} , the nematic order parameter S_N , the fraction of *trans*-conformers ϕ_{trans} , and the distance between the ends of the H_{ee} chains of paraffin were determined. The values of these characteristics for the studied systems are shown in Table VI.

Significant increase of the nematic order parameter S_N for paraffin in mixture with P3HT in comparison with pure paraffin shows that, indeed, addition of P3HT leads to increase in the degree of ordering of paraffin chains, though the average number of domains in structure of paraffin appears somewhat higher for the systems, containing P3HT, which confirms a general decrease in the degree of crystallinity of the blends. At the same time, the distance

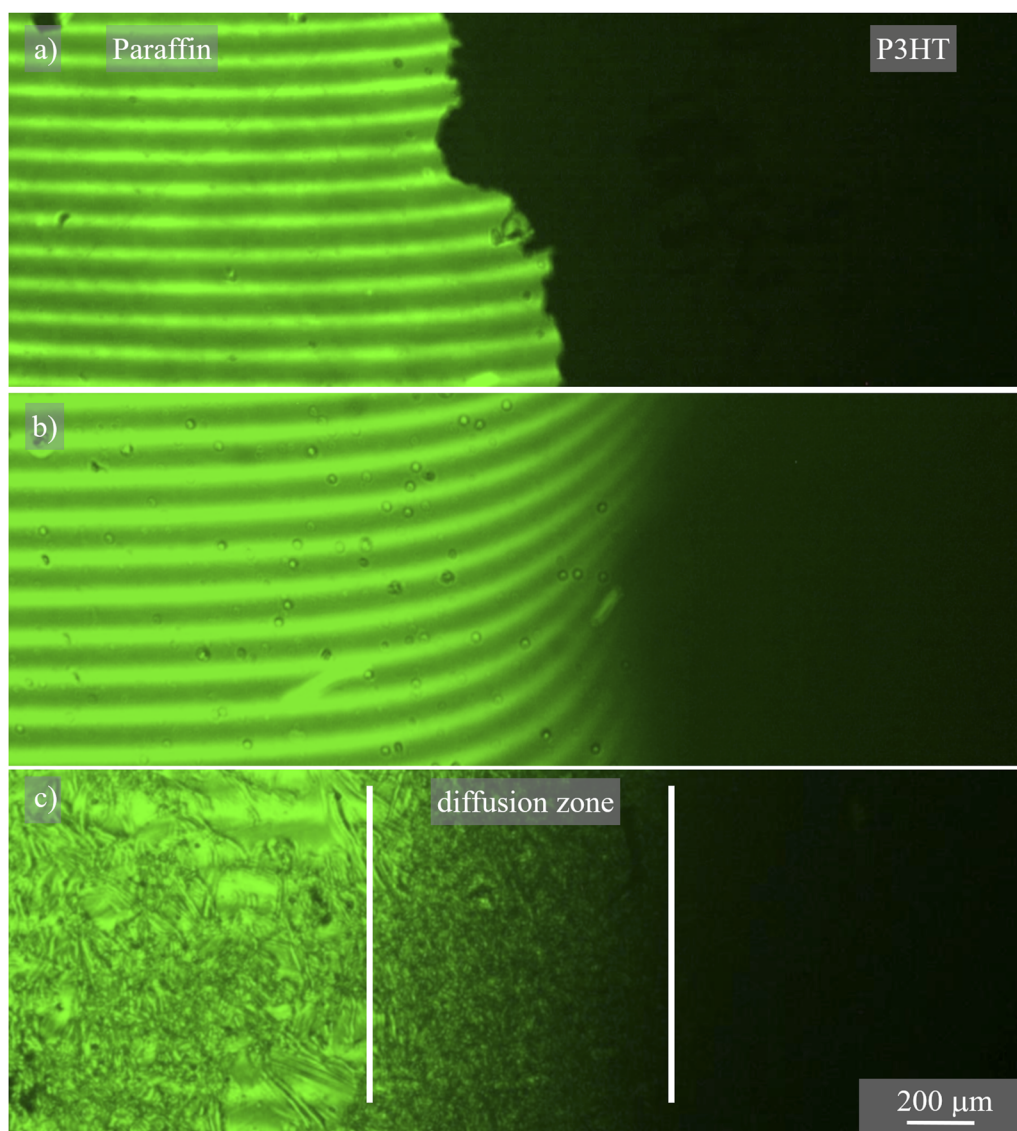


FIG. 6. Interferograms of the paraffin–P3HT system obtained at (a) 57 °C, (b) 182 °C, and (c) 26 °C.

between the ends of the paraffin molecules is the same in the pure paraffin sample and in the system on addition of P3HT, and it is equal to the maximum possible value for *n*-eicosane, i.e., in these systems, the paraffin molecules have a maximum extended conformation, which is confirmed by a high fraction of *trans*-conformers ϕ_{trans} in both systems.

For the blends containing Asp-Core asphaltenes, the formation of a dense structure with a high degree of order in which both asphaltenes and P3HT chains are embedded in the structure of the paraffin crystal is observed. It is for these blends that the maximum order parameter for the paraffin molecules and the minimum average number of domains are observed, and the density of these

systems is determined, probably, by the maximum possible packing density of the paraffin molecules.

It should be noted that although the addition of P3HT to the blend with Asp-Core asphaltenes leads to a slight decrease in the degree of ordering of the paraffin chains in the material, the distance between the ends of the paraffin molecules and the fraction of *trans*-conformers are higher exactly for the systems containing the polymer, which indicates a more complex domain structure of paraffin in these blends.

In the systems containing asphaltenes with aliphatic side groups, a multidomain structure of paraffin containing a large number of differently directed small-volume domains is observed, which

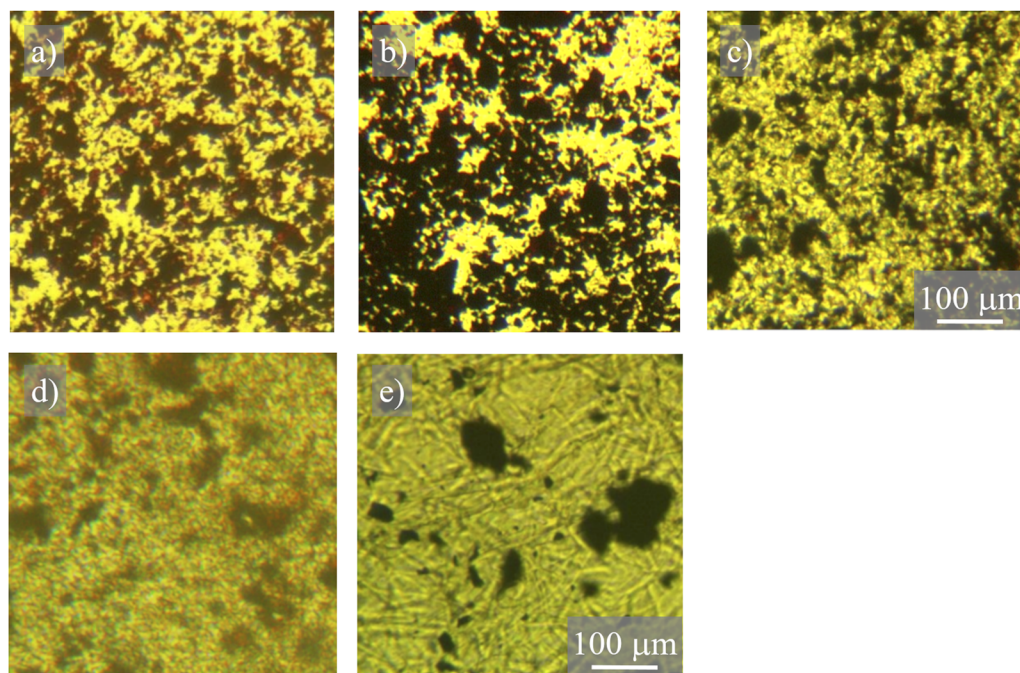


FIG. 7. Microphotographs of paraffin-based blends containing (a) 5 wt. % P3HT with the addition of 5 wt. % (b) CR-A and (c) CR-Coke (c), and blends containing only (d) 5 wt. % CR-A and (e) 5 wt. % CR-Coke at room temperature.

leads to a relatively low value of the order parameter for paraffin in these systems as well as to a lower density of the blends. Nevertheless, even in these systems, the addition of P3HT, according to computer simulation data, promotes an increase in the degree of ordering of the paraffin chains, which is expressed in an increase in their size, the fraction of *trans*-conformers, and the nematic order parameter of *n*-eicosane molecules.

To evaluate the impact of P3HT on the distribution of asphaltene molecules in paraffin-based blends, we calculated the intermolecular pair distribution functions between the aromatic asphaltene atoms $g_{A-A}(r)$ [Fig. 9(a)] and between the aromatic asphaltene atoms and the P3HT main chain atoms $g_{A-P}(r)$ [Fig. 9(b)].

A comparison of the pair distribution functions between the atoms of the aromatic nuclei of asphaltenes shows that the introduction of P3HT into the blends containing asphaltenes with aliphatic groups does not lead to changes in the pair distribution function and, accordingly, in the aggregation behavior of these asphaltenes in the blends with paraffin. Moreover, for Asp-Core asphaltenes without aliphatic groups in their composition, the pair distribution function $g_{A-A}(r)$ decreases when P3HT is added to the system, which indicates a decrease in the interaction of asphaltenes with each other, and this should lead to a decrease in the size of asphaltene aggregates. Indeed, the values of the average aggregate size of asphaltenes in the investigated systems, calculated using the built-in *clustsize* program of the Gromacs package (Table VII), show that in the systems containing Asp-Core asphaltenes, the aggregate size decreases when P3HT is added, whereas no significant change in the size of

aggregates formed by Asp-core asphaltenes occurs when P3HT is added.

Thus, the results of experimental studies and computer simulation data confirm that the introduction of P3HT into mixtures containing modified Asp-Core asphaltenes reduces the aggregation of mainly aromatic asphaltenes, which should prevent them from sedimentation in the melt.

The different influence of P3HT on the aggregation of the two considered types of asphaltenes is related to the fact that asphaltenes whose molecules contain aliphatic groups have a greater compatibility with paraffin than exclusively aromatic asphaltenes Asp-Core. In the latter case, the association of asphaltene molecules into large aggregates is facilitated by π - π interactions between the atoms of aromatic asphaltene nuclei, which, unlike asphaltenes with aliphatic groups, are not balanced by the interaction of side chains with paraffin.

P3HT has a conjugated main chain and aliphatic side chains, which ensures its compatibility with both Asp-Core aromatic asphaltene molecules and paraffin molecules, which should contribute to more uniform distribution of Asp-Core in the blends with paraffin when P3HT is introduced into them. The pairwise distribution function of the aromatic asphaltene core atoms relative to the P3HT main chain atoms $g_{A-P}(r)$ confirms the presence of specific interactions of the P3HT main chain specifically with the Asp-Core asphaltenes. In this case, $g_{A-P}(r)$ have significantly higher values than for asphaltenes with aliphatic side groups and are characterized by the presence of several peaks [Fig. 9(b)].

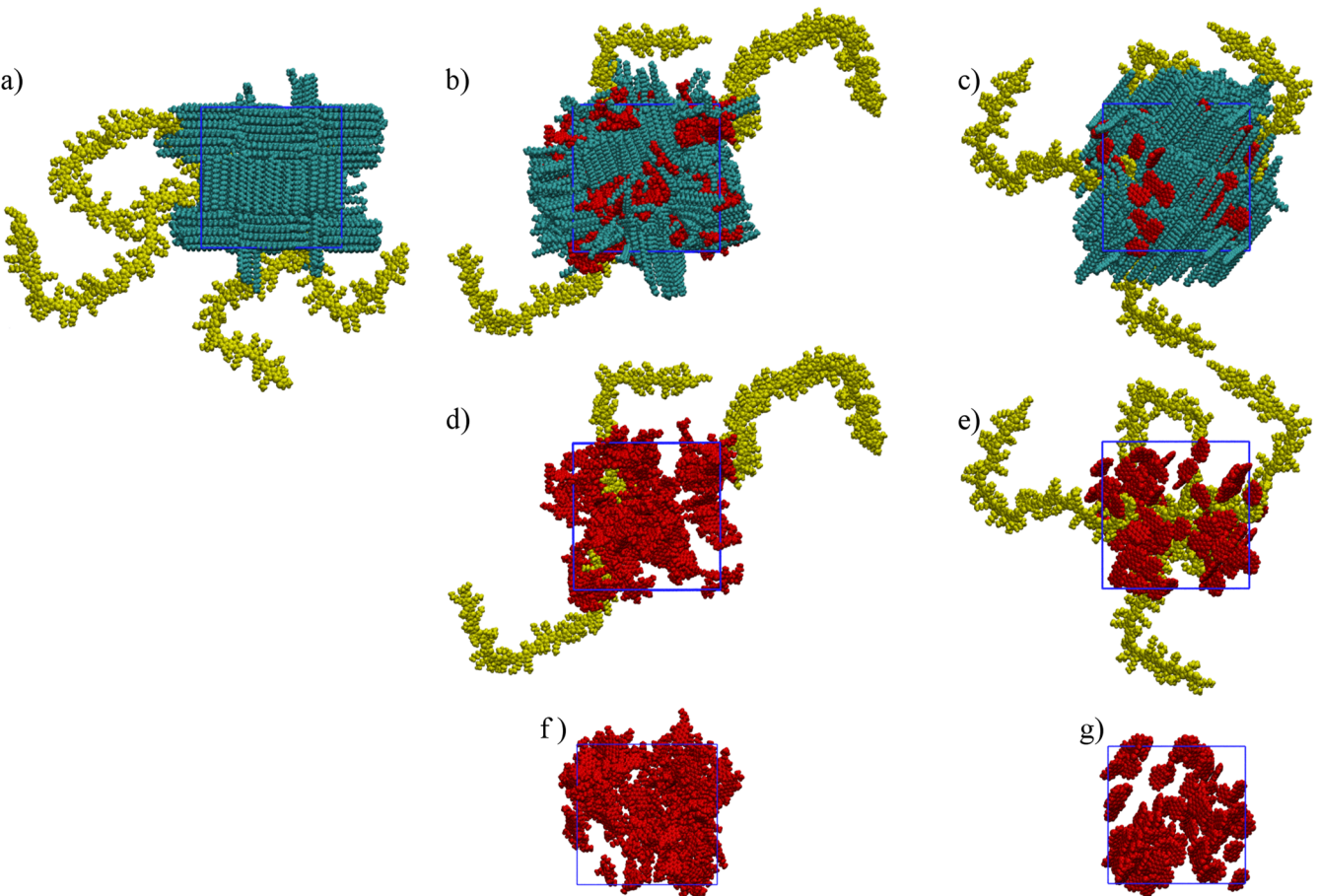


FIG. 8. Typical snapshots of the paraffin-based mixtures containing (a) P3HT, (b) and (d) P3HT and Asp, (c) and (e) P3HT and Asp-Core, (f) Asp only, and (g) Asp-Core only. Paraffin atoms are shown in cyan, P3HT atoms in yellow, and asphaltenes' atoms in red. Paraffin molecules are not shown in the panels (d)–(g) for clarity. Blue lines show a periodic simulation box.

Overall, Asp-Core molecules tend to form larger aggregates than the Asp molecules due to low compatibility of Asp-Core asphaltenes with paraffin and stronger inter-asphaltene interactions. At the same time interaction of Asp-Core asphaltenes with P3HT is higher than that of Asp, so that the polymer affects much stronger on the size of Asp-Core aggregates. As a result, we observe a considerable decrease (around 30%) in the size of Asp-Core

aggregates and almost no change in the size of Asp aggregates upon addition of P3HT (Table VII).

C. Rheological properties

It is known that molten paraffin has Newtonian fluid properties—its viscosity is independent of shear stress.⁹⁸ However,

TABLE VI. The average number of domains in the paraffin structure N_{domain} , the nematic order parameter S_N , the fraction of *trans*-conformers ϕ_{trans} , and the distance between the ends of H_{ee} paraffin molecules in the studied systems at temperature $T = -23^\circ\text{C}$.

Type of asphaltene	N_{domain}		S_N		ϕ_{trans}		H_{ee} , nm	
	With P3HT	Without P3HT	With P3HT	Without P3HT	With P3HT	Without P3HT	With P3HT	Without P3HT
No asphaltenes	4.78	3.9	0.79	0.50	0.987	0.974 ⁴³	2.43	2.43 ⁴³
Asp	18.46	19.44	0.55	0.49	0.938	0.829	2.32	2.05
Asp-core	2.73	1.36	0.95	0.98	0.983	0.961	2.43	2.37

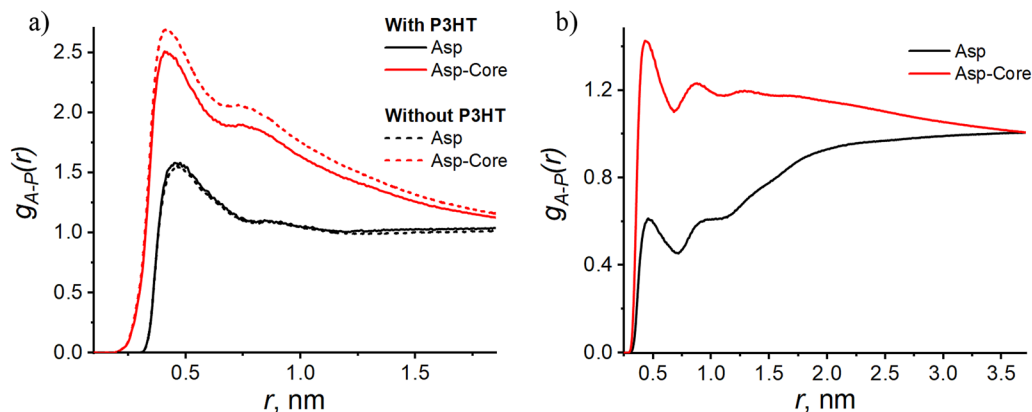


FIG. 9. The intermolecular pair distribution functions of (a) asphaltene aromatic nucleus atoms and (b) asphaltene aromatic nucleus atoms relative to P3HT main chain atoms in paraffin-based blends at $T = -23^\circ\text{C}$.

TABLE VII. Average aggregate size of asphaltenes N_{agg} in the studied systems at $T = -23^\circ\text{C}$ (the calculation was performed using the built-in *clustsize* program of the Gromacs package).

Asphaltene	With P3HT	Without P3HT
Asp	2.88 ± 0.29	2.97 ± 0.30
Asp-core	6.3 ± 1.6	8.79 ± 2.87

when 5 wt.% P3HT is introduced into the paraffin, the system exhibits an evident yield strength [Fig. 10(a)] together with increase in viscosity. This indicates that P3HT, being insoluble in the system at a temperature of 80°C , at which the measurements were made, can be considered as a filler that forms a kind of structural network in the system, which contributes to the sedimentation stability of the obtained two-component system. The enhanced sedimentation

stability can also be witnessed directly through a decrease in the sedimentation velocity of asphaltenes in paraffin when P3HT is added, see Figs. S7 and S8 in the [supplementary material](#).

At the same time, a significant increase in the yield strength for the investigated systems is observed with increasing filler concentration. If we consider the frequency dependence of the storage and loss moduli, we observe for all systems containing P3HT a very weak dependence of the moduli on the deformation frequency in the entire frequency range [Fig. 10(b)], with the storage modulus exceeding the loss modulus for all concentrations. This behavior is typical for the gel-like systems.^{99,100} It is worth noting that, as in the case of the yield strength, the values of moduli increase with increase in the filler concentration.

Note that a weak frequency dependence of the moduli is typical for so-called weak gels.^{101–103} For such gels, the relation $G''/G' > 0.1$ also holds. Obviously, both these features are present here; so, our systems can be classified as weak gels. Importantly, weak gels should

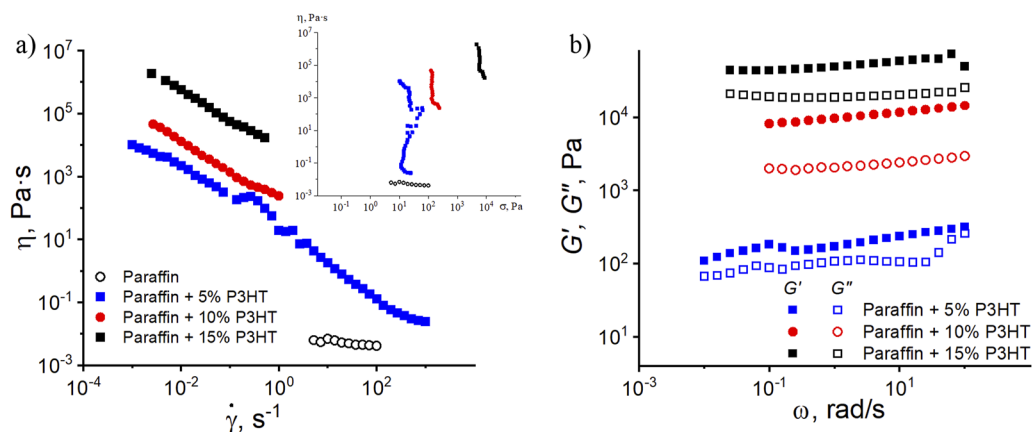


FIG. 10. Dependence of viscosity η on (a) shear rate $\dot{\gamma}$ and shear stress σ (inset in a) and (b) frequency dependence of storage and loss moduli of paraffin compositions containing P3HT (polymer concentration is indicated in the legend inside the figure), $T = 80^\circ\text{C}$.

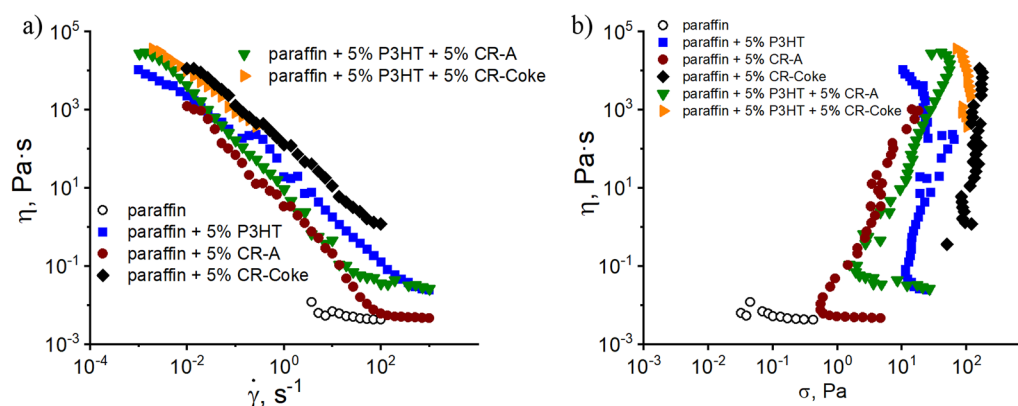


FIG. 11. Dependence of viscosity η on (a) shear rate $\dot{\gamma}$ and (b) shear stress σ for paraffin filled with P3HT and asphaltenes of different nature, $T = 80^\circ\text{C}$. The concentration of the fillers is given in the legend.

be distinguished from so-called strong gels, for which the moduli do not depend on the deformation frequency.

Thus, the introduction of poly(3-hexylthiophene) into paraffin leads to an increase in the viscosity of the system. In addition, the introduced filler forms a kind of “structural network” in the composition, the presence of which is confirmed by rheological data. Furthermore, this “network” can help prevent sedimentation of asphaltene particles.

The addition of 5 wt. % CR-A asphaltenes into the paraffin without P3HT leads to a certain structural ordering, as in the case of P3HT, because the viscosity vs shear rate relationship of such a system is at an angle close to 45° [Fig. 11(a)], and on the curve for the effective viscosity vs shear stress relationship we can observe a vertical constant stress section corresponding to the yield strength [Fig. 11(b)]. As the shear rate increase, however, this system is capable of flowing with a viscosity close to that of pure paraffin. If 5 wt. % CR-Coke asphaltenes are added to the paraffin, they are also capable of forming a “structural network,” but the yield strength of this system is significantly higher than that of similar systems with CR-A asphaltenes. This may be due to the higher stiffness of the coke asphaltene particles.

If we add asphaltenes of different nature as an additive in the paraffin containing 5 wt. % P3HT, the yield stress of such systems is determined mainly by asphaltenes. The presence of P3HT has little effect on the viscoelastic behavior of such systems.

As for the frequency and amplitude dependence of the storage and loss moduli for paraffins containing asphaltenes of different structures as fillers, as in the case of P3HT, the storage modulus exceeds the loss modulus over the entire frequency range and is independent of the deformation frequency (Fig. S9 in the [supplementary material](#)). While the concentration of the filler in the system increases, the storage modulus increases, and the systems with CR-Coke asphaltenes have higher modulus values than those containing CR-A.

Thus, the introduction of fillers into paraffin leads to the appearance of a stable supramolecular structure characterized by the value of yield strength and gel-like behavior. In this case, the highest value of both the yield strength and the storage modulus is achieved for the systems containing CR-Coke asphaltenes as a modifier.

To assess the dynamic characteristics of the investigated systems, the translational mobility of paraffin and asphaltene molecules in the blends was analyzed in computer simulations, for which the diffusion coefficients of paraffin molecules, D_{paraff} , and asphaltene, D_{asph} , in the studied systems were determined at temperature $T = 177^\circ\text{C}$ (Table VIII). It was found that the addition of a polymer in the blends with asphaltenes leads to a decrease in the mobility of paraffin and asphaltene molecules. The mobility of both asphaltenes and paraffin molecules is minimal in the systems with asphaltenes containing aliphatic side groups. The decrease in mobility of asphaltenes in the presence of poly(3-hexylthiophene) may be

TABLE VIII. Diffusion coefficients of paraffin molecules, D_{paraff} , and asphaltenes, D_{asph} , in the considered systems.

Type of asphaltene	$D_{\text{paraff}}, 10^{-5} \text{ cm}^2/\text{s}$		$D_{\text{asph}}, 10^{-5} \text{ cm}^2/\text{s}$	
	With P3HT	Without P3HT	With P3HT	Without P3HT
Without asphaltenes	2.1 ± 0.03	2.6 ± 0.03
Asp	1.4 ± 0.02	1.8 ± 0.01	0.4 ± 0.01	0.5 ± 0.04
Asp-core	1.7 ± 0.04	2.0 ± 0.2	1.1 ± 0.05	1.7 ± 0.02

directly related to the fact that the addition of P3HT increases the viscosity of the paraffin sample, which, in turn, may prevent the sedimentation of asphaltenes. Indeed, calculation of the viscosity of the paraffin/P3HT systems at 177 °C based on the computer simulation results showed a significant increase in the viscosity of the blend to 1.82 mPa s compared to that of unfilled paraffin (0.42 mPa s).⁴³

D. Thermal conductivity

The value of thermal conductivity of P3HT at room temperature, obtained using a KITT-Nanocomposite device, on a sample representing a tablet of manually compacted powder was 0.19 W/m K. Addition of 1 wt. % of P3HT to the paraffin leads to 7.2% increase in the thermal conductivity (from 0.209 to 0.224 W/m K). Then at 5 and 10 wt. % of P3HT there is a decrease to the value

0.201 W/m K (3.8 %) and at addition of 15 wt. % of P3HT leads again to 5.2% increase to 0.220 W/m K in comparison with the thermal conductivity of the paraffin (Fig. 12). The addition of 5 wt. % of asphaltenes into the blends with 5 wt. % of P3HT leads to a decrease in the thermal conductivity of the blend by 1.5% to 0.198 W/m K in the case of CR-A and to an increase by 3.6% to 0.208 W/m K in the case of CR-Coke. Thus, the introduction of P3HT with thermal conductivity close to that of paraffin does not result in any significant change in heat transfer. The introduction of P3HT to blends with asphaltenes also does not produce special results.

Modeling of the thermal conductivity of paraffin-based blends containing different types of asphaltenes (Fig. 13) showed that the introduction of P3HT into pure paraffin leads to some decrease in the thermal conductivity of the blends both in the molten (at 177 °C) and in the crystallized (at –23 °C) state. The addition of

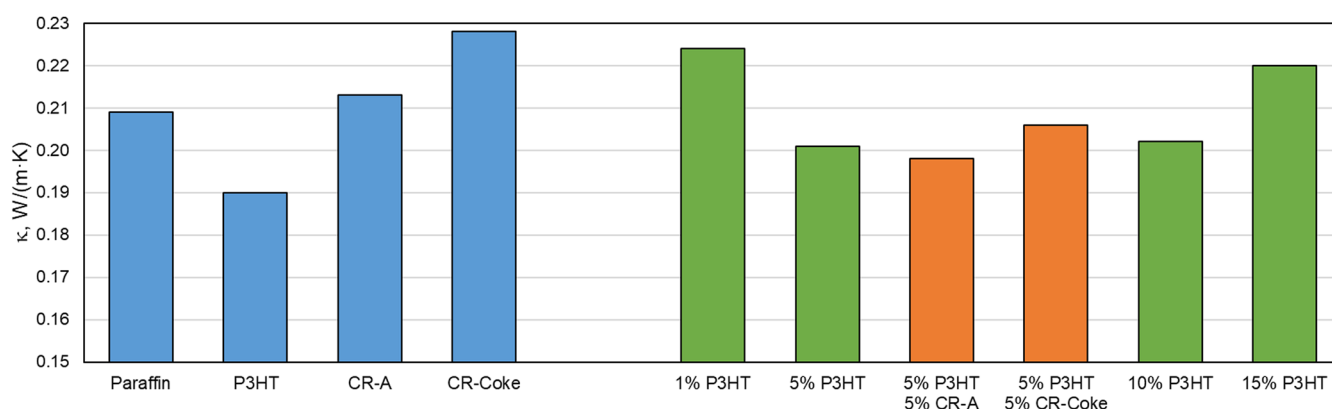


FIG. 12. Thermal conductivity of pure components of paraffin-based PCMs (blue bars), blends of paraffin with P3HT (green bars), and ternary blends containing 5 wt. % of P3HT and different types of asphaltenes (orange bars).

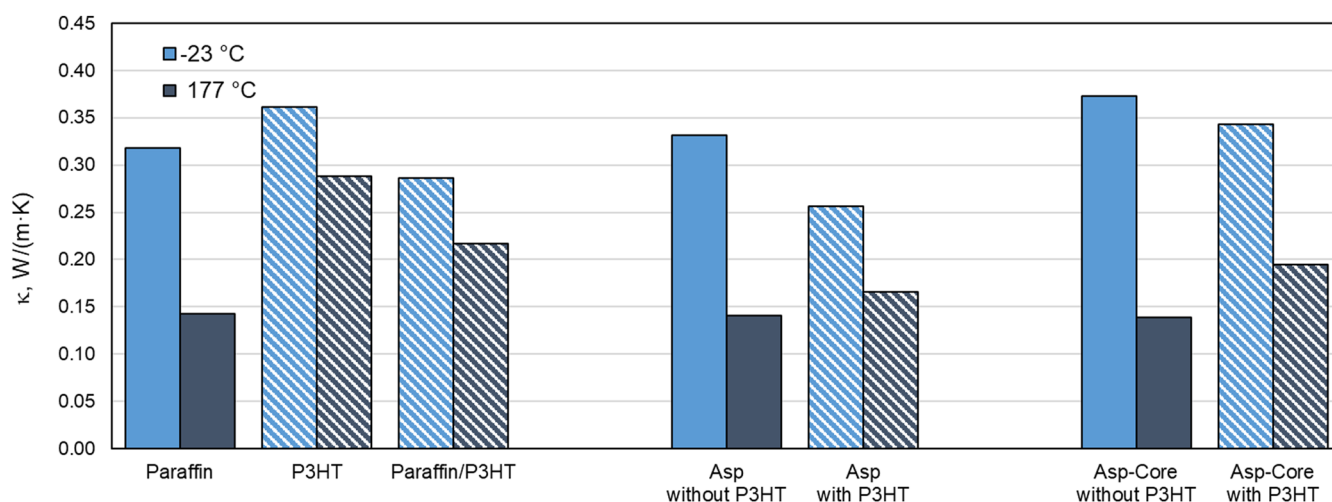


FIG. 13. Thermal conductivity of paraffin, P3HT, and their blends with asphaltenes in the molten ($T = 177$ °C, dark blue bars) and crystallized ($T = -23$ °C, light blue bars) states obtained by atomistic modeling. The patterned bars correspond to the systems comprising P3HT.

P3HT to the blends containing either Asp or Asp-Core asphaltenes slightly increases the thermal conductivity of the melt at 177 °C, but the thermal conductivity of the blend in crystallized state is lower than that before the addition of P3HT.

IV. CONCLUSIONS

The introduction of carbon nanoparticles into paraffin-based phase change materials (PCMs) is one of the most common ways to increase their thermal conductivity, which is necessary to increase the efficiency and expand the possible applications of such PCMs. The aggregation of nanoparticles in the blends with paraffins occurs due to π - π interactions, which can have multidirectional impacts on the PCM properties. On the one hand, aggregation of nanoparticles can lead to the desired increase in thermal conductivity of the blends when ordered structures are formed from the aromatic fragments of carbon nanoparticles or the formation of percolation cluster when the concentration of nanoparticles is increased, but on the other hand, it reduces the sedimentation stability of blends and can cause phase separation of PCM at temperatures above their melting point, which is undesirable.

The sedimentation and aggregation stability of nanoparticles in the blends with paraffin can be increased by introducing a small amount of agents that enhance the compatibility of aromatic fragments of carbon nanoparticles with aliphatic paraffins. Such agents can be polymers with a conjugated aromatic main chain and aliphatic side groups, such as polyalkylthiophenes, one of the best-known representatives of which is poly(3-hexylthiophene) (P3HT). Such polymers, in addition to increasing the compatibility of carbon nanofillers with paraffin, can also contribute to some increase in the thermal conductivity of PCM by forming heat transfer pathways between aggregates of nanoparticles.

In this study, using experimental and theoretical methods, a systematic study of the effect of P3HT addition on the structure and properties of promising phase change materials based on paraffin filled with asphaltenes—natural nanoparticles with an aromatic polycyclic nucleus—was carried out. In particular, the effect of P3HT on the crystallization of both pure paraffin and paraffin in blends with asphaltenes was considered, the changes in the rheological and thermal physical properties as well as the thermal conductivity of blends upon addition of P3HT were determined.

The result of this study shows that the addition of P3HT leads to a change in the rheological properties of paraffin-based systems, including an increase in their viscosity, which provides greater resistance of the blends of paraffin with asphaltenes to the sedimentation of filler particles. This is also confirmed by a decrease in the size of aggregates formed by asphaltenes in the investigated systems, both in the experiment and in atomistic computer simulations.

It was shown that in the ternary systems of paraffin/asphaltene/P3HT, co-crystallization of components is observed, which is confirmed by both experimental data and computer simulation data. Based on the analysis of the crystallization heat of these blends, it was found that the addition of P3HT to the paraffin-asphaltene blend leads to a decrease in the degree of crystallinity of the blend. However, the effect of P3HT on crystallinity is markedly inferior to the impact of asphaltenes (especially with aliphatic chains) on the crystallinity of paraffin.

According to the experimental data, the introduction of P3HT into the blend in amounts up to 15 wt. % does not significantly change the phase change temperatures of the heat-accumulating materials and does not lead to a significant change in the thermal conductivity of the materials. In turn, computer simulation showed that the blends based on paraffin and P3HT with model asphaltene molecules containing no aliphatic groups have a higher thermal conductivity compared to the blends without P3HT as well as to the blends containing asphaltene with aliphatic groups.

Thus, in this study, using a combination of experimental and computational methods, it was demonstrated that the use of small amounts of the P3HT polymer as an additive to materials for thermal storage devices based on mixtures of paraffins with asphaltene molecules leads to an increase in the sedimentation stability of the blends in liquid state, associated with an increase in their viscosity and formation of a supramolecular structure. At the same time, the addition of P3HT does not significantly affect the temperature and phase change heat of the investigated systems, and it does not impair their thermal conductivity. Thus, addition of the P3HT polymer (as well as, apparently, its more irregular analog) leads to an overall improvement in the performance of PCMs.

SUPPLEMENTARY MATERIAL

See the [supplementary material](#) for information on the characterization of asphaltene, details of the P3HT force field used for computer simulation, estimation of equilibration times in molecular dynamics simulations, DSC thermograms of P3HT, report on the sedimentation study of paraffin-asphaltene mixtures, and frequency dependence of the storage and loss moduli of paraffin-based mixtures.

ACKNOWLEDGMENTS

This research was performed with financial support from the Russian Science Foundation (Project No. 19-13-00178). The authors thank I. S. Levin for registering x-ray diffractograms in the Shared Research Center “Analytical center of deep oil processing and petrochemistry of TIPS RAS.” Computer simulations were performed using the computational resources of the Institute of Macromolecular Compounds, Russian Academy of Sciences, the equipment of the shared research facilities of HPC computing resources at Lomonosov Moscow State University, the resources of the Federal collective usage center “Complex for Simulation and Data Processing for Mega-science Facilities” at the NRC “Kurchatov Institute” (<http://ckp.nrcki.ru/>), and supercomputers at Joint Supercomputer Center of the Russian Academy of Sciences (JSCC RAS).

AUTHOR DECLARATIONS

Conflict of Interest

The authors have no conflicts to disclose.

Author Contributions

The manuscript was written through contribution of all authors. All authors have given approval of the final version of the manuscript.

Sergey V. Larin: Conceptualization (equal); Investigation (equal); Writing – original draft (equal); Writing – review & editing (equal). **Veronika V. Makarova:** Investigation (equal); Methodology (equal); Visualization (equal); Writing – original draft (equal); Writing – review & editing (equal). **Svetlana N. Gorbacheva:** Investigation (equal); Visualization (equal); Writing – original draft (equal); Writing – review & editing (equal). **Makhmut R. Yakubov:** Data curation (equal); Investigation (equal); Visualization (equal); Writing – review & editing (equal). **Sergey V. Antonov:** Conceptualization (equal); Data curation (equal); Supervision (equal); Writing – review & editing (equal). **Natalia I. Borzdun:** Investigation (equal); Visualization (equal); Writing – review & editing (equal). **Artyom D. Glova:** Investigation equal, Visualization (equal); Writing – review & editing (equal). **Victor M. Nazarychev:** Investigation (equal); Methodology (equal); Visualization (equal); Writing – review & editing (equal). **Andrey A. Gurtovenko:** Conceptualization (equal); Funding acquisition (equal); Project administration (equal); Supervision (equal); Writing – review & editing (equal). **Sergey V. Lyulin:** Conceptualization (equal); Supervision (equal); Writing – review & editing (equal).

DATA AVAILABILITY

The data that support the findings of this study are available from the corresponding author upon reasonable request.

REFERENCES

- H. Nazir, M. Batool, F. J. Bolivar Osorio, M. Isaza-Ruiz, X. Xu, K. Vignarooban, P. Phelan, Inamuddin, and A. M. Kannan, *Int. J. Heat Mass Transfer* **129**, 491 (2019).
- Z. A. Qureshi, H. M. Ali, and S. Khushnood, *Int. J. Heat Mass Transfer* **127**, 838 (2018).
- Y. Lin, Y. Jia, G. Alva, and G. Fang, *Renewable Sustainable Energy Rev.* **82**, 2730 (2018).
- V. V. Makarova, S. N. Gorbacheva, S. V. Antonov, and S. O. Ilyin, *Russ. J. Appl. Chem.* **93**, 1796 (2020).
- B. Zalba, J. M. Marin, L. F. Cabeza, and H. Mehling, *Appl. Therm. Eng.* **23**, 251 (2003).
- I. Sarbu and C. Sebarhievici, *Sustainability* **10**, 191 (2018).
- K. Pielichowska and K. Pielichowski, *Prog. Mater. Sci.* **65**, 67 (2014).
- A. Sharma, V. V. Tyagi, C. R. Chen, and D. Buddhi, *Renewable Sustainable Energy Rev.* **13**, 318 (2009).
- S. Himran, A. Suwono, and G. A. Mansoori, *Energy Sources* **16**, 117 (1994).
- S. Gschwander, S. Niedermaier, S. Gamsch, M. Kick, F. Klünder, and T. Haussmann, *Appl. Sci.* **11**, 3612 (2021).
- A. Abhat, S. Aboul-Enein, and N. A. Malatidis, *Thermal Storage of Solar Energy* (Springer Netherlands, Dordrecht, 1981), pp. 157–171.
- Y. Cui, C. Liu, S. Hu, and X. Yu, *Sol. Energy Mater. Sol. Cells* **95**, 1208 (2011).
- A. Karaipekli, A. Biçer, A. Sarı, and V. V. Tyagi, *Energy Convers. Manage.* **134**, 373 (2017).
- B. Xu and Z. Li, *Energy* **72**, 371 (2014).
- M. Amin, N. Putra, E. A. Kosasih, E. Prawiro, R. A. Luanto, and T. M. I. Mahlia, *Appl. Therm. Eng.* **112**, 273 (2017).
- X. Liu and Z. Rao, *Thermochim. Acta* **647**, 15 (2017).
- P. Goli, S. Legedza, A. Dhar, R. Salgado, J. Renteria, and A. A. Balandin, *J. Power Sources* **248**, 37 (2014).
- M. Li, *Appl. Energy* **106**, 25 (2013).
- S. Srinivasan, M. S. Diallo, S. K. Saha, O. A. Abass, A. Sharma, and G. Balasubramanian, *Int. J. Heat Mass Transfer* **114**, 318 (2017).
- A. Ohayon-Lavi, A. Lavi, A. Alatawna, E. Ruse, G. Ziskind, and O. Regev, *Renewable Energy* **167**, 580 (2021).
- Y. Zhao, L. Jin, B. Zou, G. Qiao, T. Zhang, L. Cong, F. Jiang, C. Li, Y. Huang, and Y. Ding, *Appl. Therm. Eng.* **171**, 115015 (2020).
- V. V. Makarova, S. N. Gorbacheva, A. V. Kostyuk, S. V. Antonov, Y. Y. Borisova, D. N. Borisov, and M. R. Yakubov, *J. Energy Storage* **47**, 103595 (2022).
- A. D. Glova, V. M. Nazarychev, S. V. Larin, A. V. Lyulin, S. V. Lyulin, and A. A. Gurtovenko, *J. Mol. Liq.* **346**, 117112 (2022).
- H. Zhang, T. Shi, and A. Ma, *Polymers* **13**, 2797 (2021).
- H. Zheng, K. Wu, W. Chen, B. Nan, Z. Qu, and M. Lu, *Macromol. Chem. Phys.* **222**, 2000418 (2021).
- U. Mehmood, A. Al-Ahmed, and I. A. Hussein, *Renewable Sustainable Energy Rev.* **57**, 550 (2016).
- A. R. Murad, A. Iraqi, S. B. Aziz, S. N. Abdullah, and M. A. Brza, *Polymers* **12**, 2627 (2020).
- S. Günes, H. Neugebauer, and N. S. Sariciftci, *Chem. Rev.* **107**, 1324 (2007).
- B. Mei, Y. Qin, and S. Agbolaghi, *Solar Energy* **215**, 77 (2021).
- J. A. Hauch, P. Schilinsky, S. A. Choulis, R. Childers, M. Biele, and C. J. Brabec, *Sol. Energy Mater. Sol. Cells* **92**, 727 (2008).
- U. K. Bhui, A. Ray, and M. P. Joshi, *Macromolecular Characterization of Hydrocarbons for Sustainable Future* (Springer Singapore, 2021), pp. 129–139.
- N. I. Borzdun, R. R. Ramazanov, A. D. Glova, S. V. Larin, and S. V. Lyulin, *Energy Fuels* **35**, 8423 (2021).
- S. Peng, A. Fuchs, and R. A. Wirtz, *J. Appl. Polym. Sci.* **93**, 1240 (2004).
- O. C. Mullins, *Annu. Rev. Anal. Chem.* **4**, 393 (2011).
- M. Kamkar and G. Natale, *Fuel* **285**, 119272 (2021).
- E. M. Deemer and R. R. Chianelli, *Modified Asphalt* (InTech, 2018).
- R. E. Abujnah, H. Sharif, B. Torres, K. Castillo, V. Gupta, and R. R. Chaielli, *J. Environ. Anal. Toxicol.* **06**, 1000345 (2016).
- B. D. Babaev, *High Temp.* **52**, 736 (2014).
- A. Y. Malkin and A. E. Chalykh, *Diffusion and Viscosity of Polymers: Measurement Techniques* (Khimia, Moscow, 1979).
- V. Makarova and V. Kulichikhin, *Interferometry—Research and Applications in Science and Technology* (InTech, 2012).
- S. N. Gorbacheva, V. V. Makarova, and S. O. Ilyin, *J. Energy Storage* **36**, 102417 (2021).
- J. Paris, M. Falardeau, and C. Villeneuve, *Energy Sources* **15**, 85 (1993).
- A. D. Glova, I. V. Volgin, V. M. Nazarychev, S. V. Larin, S. V. Lyulin, and A. A. Gurtovenko, *RSC Adv.* **9**, 38834 (2019).
- V. M. Nazarychev, A. D. Glova, I. V. Volgin, S. V. Larin, A. V. Lyulin, S. V. Lyulin, and A. A. Gurtovenko, *Int. J. Heat Mass Transfer* **165**, 120639 (2021).
- I. V. Volgin, A. D. Glova, V. M. Nazarychev, S. V. Larin, S. V. Lyulin, and A. A. Gurtovenko, *RSC Adv.* **10**, 31316 (2020).
- T. Liu, D. L. Cheung, and A. Troisi, *Phys. Chem. Chem. Phys.* **13**, 21461 (2011).
- M. Bernardi, M. Giulianini, and J. C. Grossman, *ACS Nano* **4**, 6599 (2010).
- Y. Y. Yimer and M. Tsige, *J. Chem. Phys.* **137**, 204701 (2012).
- N. I. Borzdun, S. V. Larin, S. G. Falkovich, V. M. Nazarychev, I. V. Volgin, A. V. Yakimansky, A. V. Lyulin, V. Negi, P. A. Bobbert, and S. V. Lyulin, *J. Polym. Sci., Part B: Polym. Phys.* **54**, 2448 (2016).
- B. Schuler, G. Meyer, D. Peña, O. C. Mullins, and L. Gross, *J. Am. Chem. Soc.* **137**, 9870 (2015).
- S. V. Lyulin, A. D. Glova, S. G. Falkovich, V. A. Ivanov, V. M. Nazarychev, A. V. Lyulin, S. V. Larin, S. V. Antonov, P. Ganani, and J. M. Kenny, *Pet. Chem.* **58**, 983 (2018).
- E. S. Boek, D. S. Yakovlev, and T. F. Headen, *Energy Fuels* **23**, 1209 (2009).
- D. D. Li and M. L. Greenfield, *Fuel* **115**, 347 (2014).
- T. F. Headen, E. S. Boek, and N. T. Skipper, *Energy Fuels* **23**, 1220 (2009).
- T. F. Headen, E. S. Boek, G. Jackson, T. S. Totton, and E. A. Müller, *Energy Fuels* **31**, 1108 (2017).
- A. D. Glova, S. V. Larin, V. M. Nazarychev, J. M. Kenny, A. V. Lyulin, and S. V. Lyulin, *ACS Omega* **4**, 20005 (2019).
- M. B. Singh, N. Rampal, and A. Malani, *Energy Fuels* **32**, 8259 (2018).

- ⁵⁸Z. Dong, Z. Liu, P. Wang, and X. Gong, *Fuel* **189**, 155 (2017).
- ⁵⁹M. Xu, J. Yi, P. Qi, H. Wang, M. Marasteanu, and D. Feng, *Energy Fuels* **33**, 1387 (2019).
- ⁶⁰T. Emrick and E. Pentzer, *NPG Asia Mater.* **5**, e43 (2013).
- ⁶¹G. Kiršanskas, Q. Li, K. Flensburg, G. C. Solomon, and M. Leijnse, *Appl. Phys. Lett.* **105**, 233102 (2014).
- ⁶²O. C. Mullins, H. Sabbah, J. Eyssautier, A. E. Pomerantz, L. Barré, A. B. Andrews, Y. Ruiz-Morales, F. Mostowfi, R. McFarlane, L. Goual, R. Lepkowitz, T. Cooper, J. Orbulescu, R. M. Leblanc, J. Edwards, and R. N. Zare, *Energy Fuels* **26**, 3986 (2012).
- ⁶³R. Dutta Majumdar, T. Montana, O. C. Mullins, M. Gerken, and P. Hazendonk, *Fuel* **193**, 359 (2017).
- ⁶⁴J. A. Duran, Y. A. Casas, L. Xiang, L. Zhang, H. Zeng, and H. W. Yarranton, *Energy Fuels* **33**, 3694 (2019).
- ⁶⁵H. Bian, F. Xu, A. Kan, S. Wei, H. Zhang, S. Zhang, L. Zhu, and D. Xia, *J. Mol. Liq.* **343**, 117576 (2021).
- ⁶⁶A. H. Alshareef, K. Azyat, R. R. Tykwinski, and M. R. Gray, *Energy Fuels* **24**, 3998 (2010).
- ⁶⁷H. M. S. Lababidi, H. M. Sabti, and F. S. AlHumaidan, *Fuel* **117**, 59 (2014).
- ⁶⁸M. J. Abraham, T. Murtola, R. Schulz, S. Páll, J. C. Smith, B. Hess, and E. Lindahl, *SoftwareX* **1–2**, 19 (2015).
- ⁶⁹S. Páll, A. Zhmurov, P. Bauer, M. Abraham, M. Lundborg, A. Gray, B. Hess, and E. Lindahl, *J. Chem. Phys.* **153**, 134110 (2020).
- ⁷⁰D. van der Spoel, E. Lindahl, B. Hess, G. Groenhof, A. E. Mark, and H. J. C. Berendsen, *J. Comput. Chem.* **26**, 1701 (2005).
- ⁷¹J. Wang, R. M. Wolf, J. W. Caldwell, P. A. Kollman, and D. A. Case, *J. Comput. Chem.* **25**, 1157 (2004).
- ⁷²P. Venkataraman, K. Zygourakis, W. G. Chapman, S. L. Wellington, and M. Shammai, *Energy Fuels* **31**, 1182 (2017).
- ⁷³J. Xu, N. Wang, S. Xue, H. Zhang, J. Zhang, S. Xia, and Y. Han, *Fuel* **310**, 122270 (2022).
- ⁷⁴S. Obata and Y. Shimoi, *Phys. Chem. Chem. Phys.* **15**, 9265 (2013).
- ⁷⁵C. Trapalis, E. Lidorikis, and D. G. Papageorgiou, *Comput. Theor. Chem.* **1190**, 112997 (2020).
- ⁷⁶Q.-Q. Pan, Z.-W. Zhao, Y. Wu, Y. Geng, M. Zhang, and Z.-M. Su, *J. Taiwan Inst. Chem. Eng.* **100**, 160 (2019).
- ⁷⁷R. C. Pani, B. D. Bond, G. Krishnan, and Y. G. Yingling, *Soft Matter* **9**, 10048 (2013).
- ⁷⁸Q.-Q. Pan, Z.-W. Zhao, Y. Wu, and Y. Geng, *J. Mol. Graphics Modell.* **94**, 107488 (2020).
- ⁷⁹A. W. Sousa da Silva and W. F. Vranken, *BMC Res. Notes* **5**, 367 (2012).
- ⁸⁰J. Wang, W. Wang, P. A. Kollman, and D. A. Case, *J. Mol. Graphics Modell.* **25**, 247 (2006).
- ⁸¹H. J. C. Berendsen, J. P. M. Postma, W. F. van Gunsteren, A. DiNola, and J. R. Haak, *J. Chem. Phys.* **81**, 3684 (1984).
- ⁸²S. Nosé, *Mol. Phys.* **52**, 255 (1984).
- ⁸³W. G. Hoover, *Phys. Rev. A* **31**, 1695 (1985).
- ⁸⁴M. Parrinello and A. Rahman, *J. Appl. Phys.* **52**, 7182 (1981).
- ⁸⁵B. Hess, *J. Chem. Theory Comput.* **4**, 116 (2008).
- ⁸⁶U. Essmann, L. Perera, M. L. Berkowitz, T. Darden, H. Lee, and L. G. Pedersen, *J. Chem. Phys.* **103**, 8577 (1995).
- ⁸⁷V. Nazarychev, A. Glova, S. Larin, A. Lyulin, S. Lyulin, and A. Gurtovenko, *chemRxiv:2022-jcxmz* (2022).
- ⁸⁸J. Ramos, J. F. Vega, and J. Martínez-Salazar, *Macromolecules* **48**, 5016 (2015).
- ⁸⁹T. Zhang and T. Luo, *J. Phys. Chem. B* **120**, 803 (2016).
- ⁹⁰M. S. Green, *J. Chem. Phys.* **22**, 398 (1954).
- ⁹¹R. Kubo, *J. Phys. Soc. Jpn.* **12**, 570 (1957).
- ⁹²S. Plimpton, *J. Comput. Phys.* **117**, 1 (1995).
- ⁹³D. Surblys, H. Matsubara, G. Kikugawa, and T. Ohara, *Phys. Rev. E* **99**, 051301 (2019).
- ⁹⁴I. Krupa, G. Miková, and A. S. Luyt, *Eur. Polym. J.* **43**, 4695 (2007).
- ⁹⁵J. E. K. Schawe, *J. Appl. Polym. Sci.* **133**, 42977 (2016).
- ⁹⁶I. S. Kolesov, R. Androsch, and H.-J. Radusch, *J. Therm. Anal. Calorim.* **78**, 885 (2004).
- ⁹⁷V. S. Balderrama, M. Estrada, A. Viterisi, P. Formentin, J. Pallarés, J. Ferré-Borrull, E. Palomares, and L. F. Marsal, *Microelectron. Reliab.* **53**, 560 (2013).
- ⁹⁸F. Rossetti, G. Ranalli, and C. Faccenna, *J. Struct. Geol.* **21**, 413 (1999).
- ⁹⁹Y. Xu, A. D. Atrens, and J. R. Stokes, *Soft Matter* **14**, 1953 (2018).
- ¹⁰⁰S. N. Gorbacheva, Y. M. Yarmush, and S. O. Ilyin, *Tribol. Int.* **148**, 106318 (2020).
- ¹⁰¹S. Ikeda and K. Nishinari, *J. Agric. Food Chem.* **49**, 4436 (2001).
- ¹⁰²I. S. Chronakis, L. Piculell, and J. Borgström, *Carbohydr. Polym.* **31**, 215 (1996).
- ¹⁰³S. B. Ross-Murphy, V. J. Morris, and E. R. Morris, *Faraday Symp. Chem. Soc.* **18**, 115 (1983).